4: Photometry

The mathematical thermology created by Fourier may tempt us to hope that... we may in time ascertain the mean temperature of the heavenly bodies: but I regard this order of facts as forever excluded from our recognition.

Auguste Comte *Cours de la Philosophie Positive*[1] (1835)

...within a comparatively few years, a new branch of astronomy has arisen which studies the sun, moon, and stars for what they are in themselves and in relation to ourselves.

Samuel Pierpont Langley *The New Astronomy* (1888)

Purpose

In 1835 the French philosopher Auguste Comte noted that since we know stars only by their light (and cannot take bits of stars into the laboratory), our knowledge of stars would be forever limited essentially to location. Fifty years later astrophysics—the study of the physics of stars—was beginning, and the first measurements of the Sun's temperature and composition were being made. Evidently, careful measurement of starlight (photometry) allows the intrinsic properties of stars to be determined. In this lab you will use broadband photometry to measure the temperature of stars.

Introduction

We begin our study of stars with blackbody radiation, which you studied in Modern Physics and you will yourself measure in the Thermionic Emission lab (p. 121). The light produced by a hot object is akin to audio noise: in both cases a random process produces a simultaneous superposition of a wide distribution of wavelengths. In his *Opticks*, Newton noted certain systematic dependencies in the light emitted by incandescent objects and suggested something fundamental was behind the process[2]. Apparently the light produced by an incandescent object is fundamentally related to its temperature not its material composition. In 1879 Joseph Stefan proposed that every object emits light energy at the rate (power in

---

[1]`http://socserv2.mcmaster.ca/~econ/ugcm/3ll3/comte/` provides this as an etext translated and edited by Harriet Martineau.

[2]*Query 8*: Do not all fix'd Bodies, when heated beyond a certain degree, emit Light and shine...
Query 11:...And are not the Sun and fix'd Stars great Earths vehemently hot...

watts):

$$P = \epsilon_T \sigma T^4 \mathcal{A} \tag{4.1}$$

where σ is the Stefan-Boltzmann[3] constant, T is the absolute temperature of the body, $\mathcal{A}$ is the surface area of the body, and ϵ_T is the total emissivity.

Experimentally it was found that the wavelength distribution of the light from hot objects was broadly similar to the Maxwell-Boltzmann speed distribution: a bell-shaped curve in which the location of the peak (i.e., the most common wavelength) depended on temperature. In 1893 Wilhelm Wien[4] concluded that the wavelength of this peak must be inversely proportional to temperature. Experiment confirmed that the wavelength of this peak was given by:

$$\lambda_{max} = \frac{2898 \ \mu m \cdot K}{T} \tag{4.2}$$

Together the Stefan-Boltzmann and Wien displacement laws—both the results of classical physics—explain much of what is commonly observed in hot objects. At room temperature objects do not appear to be a source of light: they appear dark (unless externally illuminated). This is a result both of the small rate of emission given by Stefan-Boltzmann and (from Wien) for $T = 300$ K, we find $\lambda_{max} \sim 10 \ \mu m$, that is the wavelengths typically emitted are well outside the range of light that can be detected by the eye[5]. On the other hand for an object like the Sun: $T \approx 6000$ K, so $\lambda_{max} \sim 0.5 \ \mu m$ — right in the middle of of the visible range.

Our 'spherical cow' model[6] of a star is an incandescent ball (radius R) of gas shining as a blackbody. Thus the total power output of a star (called the *luminosity*[7]) is

$$L = \sigma T^4 \ 4\pi R^2 \tag{4.3}$$

The equation for the exact distribution of photon wavelengths produced by a blackbody was actively researched with erroneous equations produced by Wien and Rayleigh & Jeans. In 1900 Max Planck[8] published his derivation of the wavelength distribution of light from a blackbody. However before we can discuss his result we must explain what precisely is meant by 'wavelength distribution'.

In Physics 211 you learned about the speed distribution[9] of the molecules in a gas: a bell-shaped curve that shows that slow molecules are rare and supersonic molecules are

---

[3]In 1879 Jožef Stefan (1835–93) proposed the law based on experimental measurements; five years later Ludwig Boltzmann (1844–1906) derived the result from fundamental thermodynamics. Today the result is known as the Stefan-Boltzmann Law.

[4]Wilhelm Wien (1864–1928) German physicist, 1911 Nobel Prize in Physics

[5]The human eye can detect light with a wavelength in the range 0.4 μm (violet) to 0.7 μm (red).

[6]This model of a star works best with stars similar in temperature to the Sun, but every star's light is considerably modified by absorption as it travels through the star's atmosphere. In hot stars, UV wavelengths that can photoionize hydrogen ($H(n = 2) + \gamma \rightarrow H^+ + e^-$) are highly attenuated producing the Balmer jump. The spectra of cool stars shows broad absorption bands due to molecules. http://www.jb.man.ac.uk/distance/life/sample/java/spectype/specplot.htm is an applet allowing a comparison of blackbody light to actual star light.

[7]The MKS unit for luminosity is watt, but the numbers are so large that it is usually expressed as a multiple (or fraction) of the Sun's luminosity (a.k.a., solar luminosity) $L_\odot = 3.846 \times 10^{26}$ W.

[8]Max Planck (1858–1947) German physicist, 1918 Nobel Prize in Physics

[9]Derived by James Clerk Maxwell (1831–1879); Ludwig Boltzmann (1844–1906) provided a firm foundation for the result using statistical mechanics. Today the result is generally known as the Maxwell-Boltzmann distribution.
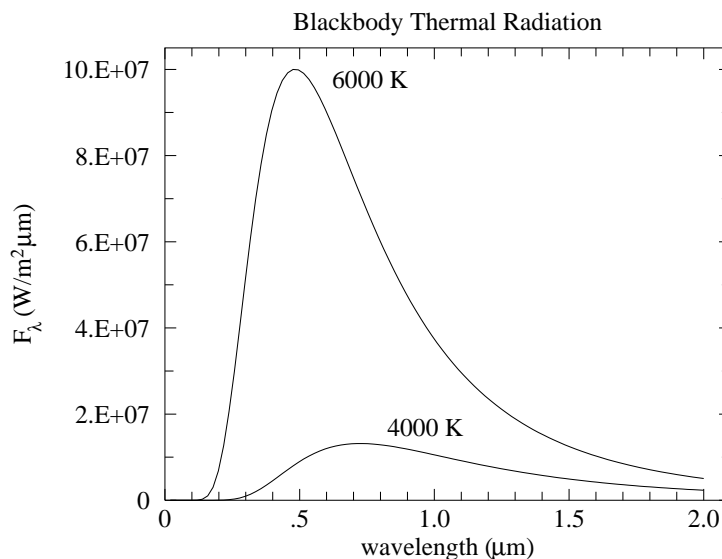
Blackbody Thermal Radiation

Figure 4.1: The distribution of the light emitted by a blackbody plotted as a function of wavelength. Hotter objects emit much more light than cool ones, particularly at the shorter wavelengths.

rare, whereas a molecular kinetic energy near $\frac{3}{2}kT$ is common. 'Speed probability' is a problematic concept. For example the probability that a molecule has a speed of exactly π m/s (or any other real number) must be essentially zero[10] (as an infinite number of digits must match, but there are only a finite [but huge] number of molecules). Probability density provides a meaningful context to talk about speed distribution: determine the fraction of molecules ('hits') that have speed in an interval (bin) $(v - \Delta v/2, v + \Delta v/2)$ for various speeds v. (Here the bin is centered on the speed v and has bin-size Δv.) Clearly the number of hits in a bin depends on the bin-size (or range), but you should expect that the hit *density* (number of hits divided by the bin-size) should be approximately independent of the bin-size. A plot of fraction-per-bin-size vs. bin center provides the usual bell-shaped curve. Bins centered on both slow and supersonic speeds include few molecules whereas bins that correspond to molecular kinetic energy near $\frac{3}{2}kT$ include a large fraction of molecules.

In a similar way we can sort the light by wavelength into a sequence of wavelength intervals (bins), and calculate the total light *energy* per bin-size. For example, if there were[11] a total of 2 J of light energy (about 5×10^{18} photons) with wavelengths in the interval (.50, .51) μm we would say the intensity of light at $\lambda = .505$ μm was about 200 J/μm. In the case of the thermal radiation continuously emitted from the surface of a body, we are interested in the *rate* of energy emission per area of the body, with units $(W/m^2)/\mu$m. This quantity is called the monochromatic flux density and denoted F_λ[12]. Planck's result was:

$$F_\lambda = \frac{2\pi h c^2}{\lambda^5} \frac{1}{\exp(hc/\lambda kT) - 1} \tag{4.4}$$

---

[10]A mathematician would say the probability is zero for *almost every* speed.

[11]These numbers correspond approximately to 0.1 sec of full sunlight on 1 m^2 of the Earth.

[12]One could just as well measure bin-size in Hz. The result is denoted F_ν with units $(W/m^2)/Hz$. A helpfully sized unit for F_ν is the jansky: 1 Jy $= 10^{-26} W \cdot m^{-2} \cdot Hz^{-1}$. F_ν is commonly used in radio astronomy whereas F_λ is commonly used in optical astronomy.

where h is Planck's constant, whose presence is a sign of the importance of quantum mechanical effects. The primary assumption in Planck's derivation of this distribution was the *photon*: an indivisible packet of light carrying total energy $E = hc/\lambda$. With this identification notice the Boltzmann factor in Planck's equation: $\exp(E/kT)$. As before, this factor means that high energy (i.e., short wavelength) photons are rarely in the mix of emitted photons. Thus only 'high' temperature stars will emit an abundance of UV radiation.

Of course, the light emitted from the surface of a star gets spread over an ever larger area as it moves away from the star. Thus the flux coming into a telescope a distance r from the center of the star would be:

$$F_\lambda = \frac{2\pi h c^2}{\lambda^5} \, \frac{R^2}{r^2} \, \frac{1}{\exp(hc/\lambda kT) - 1} \tag{4.5}$$

Theoretically it's now easy to measure the temperature of stars: simply measure the wavelength distribution ('spectra') of the starlight and fit the measurements to the above theory with two adjustable parameters: T and R/r. (Do notice that increasing R or decreasing r produces exactly the same effect—an overall increase in the flux density—so we cannot separately determine R and r from the spectra. A large, distant $T = 6000$ K star could have exactly the same spectra as a small, close $T = 6000$ K star.) Let me enumerate a few (of the many) reasons this does not work perfectly.

1. We assumed above that space was transparent: that the only effect of distance was diluting the light over a greater area. However, our Galaxy is filled with patchy clouds of dust. Unfortunately the dust in these clouds has the property of being more likely to absorb blue light than red. Thus a dust-obscured star will lose more blue than red light and the observed spectra will be distorted from that emitted. A dust-obscured star would measure cooler and appear more distant (i.e., dimmer) than it actually was. These two effects of dust are called 'reddening' and 'extinction'. Of course substantial dust absorption is more likely for more distant stars. It is usually 'small' for stars within 300 Ly of Earth. However, 300 Ly covers a very tiny fraction of our Galaxy. In this lab we will side step this problem by selecting stars with little dust absorption. However, with a bit of additional work, dust absorption could be measured and corrected for using photometry.

2. Starlight measured from the surface of the Earth must traverse the Earth's atmosphere. The non-transparency of the Earth's atmosphere will also modify the observed starlight. In addition, the telescope and detector typically introduce additional 'non-transparency', that is blue and red photons at the telescope aperture are not equally likely to be counted. The 'efficiency' of the system depends on wavelength. Unless extraordinary care is taken, this efficiency can change on a daily basis. (And, of course, the atmosphere's transparency can change in a matter of minutes.) As a result frequent calibration of the system is required. Calibration at the multitude of wavelengths required to make a full spectra is obviously more difficult than calibration at just a few wavelengths.

3. There is a competition between the accurate measurement of the value of F_λ and the bin-size used. As you may have noticed in the Bubble Chamber lab, if you select a small bin-size, each bin captures relatively few hits which results in relatively large $\sqrt{N}$ errors. So if you have only a few thousand photons, you may do better to use a big bin-size (so you capture enough counts to get an accurate measurement of F_λ),

but then only have a few bins (each spanning a large interval of in wavelength) so, unfortunately, the spectrum has been reduced to just a few points. Of course, you could always collect starlight for a longer period of time (longer 'integration time') or use a telescope with a larger aperture. However, these solutions miss the point: The boundary between the known and unknown in astronomy is almost always at the edge of what you can just barely detect. Thus you must always come up with the maximally efficient use of the available photons. Telescope time is allocated for a detailed spectra only when it is expected that the results cannot be obtained in a 'cheaper' way.

4. Stars are not exact blackbodies, and of course they are not at <u>a</u> temperature. Certainly if we move from the surface to core of a star we would experience quite different temperatures. But even on the 'surface' of our Sun we see regions ('sunspots') with unusually low temperature. In the Langmuir Probe lab, you will find that the electrons in a tube of gas may have a different temperature from the co-mingled atoms. Similarly, in the atmospheres of stars it is not unusual for the various components of the gas to be at different temperatures (that is to say the gas is not in local thermodynamic equilibrium [LTE]). Hence it may make no sense to try to obtain high-precision measurements of 'the' temperature.

Oddly enough the fact that stars are not blackbodies is actually helpful as it allows a variety of information to be decoded from the starlight. (A blackbody spectra includes just two bits of information the temperature T and R/r.) Varying absorption in the star's atmosphere means that some light (i.e., λ at which the star's atmosphere is largely transparent) comes from deeper in the star and hence represents a higher temperature. Ultimately the absorption lines in a star's spectra provide the bulk of the information we have about stars. Chemical composition of the star's atmosphere and temperature—accurate[13] to a few percent—are best obtained this way. However, consideration of these absorption lines is beyond the aims of this lab.

Temperature I

Your aim in this lab is to measure the temperature of stars without resorting to a detailed measurement of the star's spectra. We begin by considering measurement of F_λ at just two wavelengths: F_1 at λ_1 and F_2 at λ_2 where $\lambda_1 < \lambda_2$. (Think of λ_1 as blue light and λ_2 as red light.) There is a huge cancellation of factors if we look at the ratio: F_2/F_1:

$$\frac{F_2}{F_1} = \frac{\lambda_1^5}{\lambda_2^5} \frac{\exp(hc/\lambda_1 kT) - 1}{\exp(hc/\lambda_2 kT) - 1} \tag{4.6}$$

In general, ratios are great things to measure because (A) since they are dimensionless they are more likely to be connected to intrinsic properties and (B) it is often the case that systematic measurement errors will (at least in part) cancel out in a ratio. For starlight, the flux will depend on distance ($\propto 1/r^2$), but in a flux ratio the effects of distance will (in theory) cancel out.

---

[13]Statements like this—that imply we know the true accuracy of our measurements—should be read with the knowledge that history shows unexpected jumps in results as systematic errors are discovered. The history of the measured chemical composition of stars would show graphs much like those in Figure 1 on page 10.

While the ratio has considerably reduced the complexity of the formula, it would help if we had an even simpler formula. Towards that goal we make the approximation that the exponential terms are much larger than 1:

$$\frac{F_2}{F_1} = \frac{\lambda_1^5}{\lambda_2^5} \frac{\exp(hc/\lambda_1 kT) - 1}{\exp(hc/\lambda_2 kT) - 1} \tag{4.7}$$

$$\approx \frac{\lambda_1^5}{\lambda_2^5} \frac{\exp(hc/\lambda_1 kT)}{\exp(hc/\lambda_2 kT)} = \frac{\lambda_1^5}{\lambda_2^5} \exp\left[\frac{hc}{kT}\left(\frac{1}{\lambda_1} - \frac{1}{\lambda_2}\right)\right] \tag{4.8}$$

$$\log(F_2/F_1) \approx \frac{hc}{kT}\left(\frac{1}{\lambda_1} - \frac{1}{\lambda_2}\right)\log e + 5\log(\lambda_1/\lambda_2) \tag{4.9}$$

Example

Consider the case where $\lambda_1 = .436$ μm (blue) and $\lambda_2 = .545$ μm (green or 'visible'). For historical reasons, astronomers prefer to consider $2.5\log_{10}(F_2/F_1)$, and if we evaluate all of the constants we find:

$$2.5\log_{10}(F_2/F_1) \approx \frac{7166 \text{ K}}{T} - 1.21 \tag{4.10}$$

Do notice that for cool stars this quantity is large (more 'visible' than blue light) and that extremely hot stars ($T \to \infty$) will all have much the same value for this quantity: -1.21. This last result is a consequence of the 'Rayleigh-Jeans' approximation for the Planck distribution, valid for $\lambda \gg \lambda_{max}$. In this large wavelength (or high temperature) limit, the Boltzmann factors are nearly one and:

$$\exp(hc/\lambda kT) - 1 \approx hc/\lambda kT \tag{4.11}$$

so[14]

$$F_\lambda \approx \frac{2\pi hc^2}{\lambda^5} \frac{\lambda kT}{hc} = kT\frac{2\pi c}{\lambda^4} \tag{4.12}$$

Since temperature is now an over-all factor, it will cancel out in any flux ratio.

Color Index

At increasing distance from the star, both F_2 and F_1 will be diminished, but by exactly the same fraction (assuming space is transparent, or at least not colored). Thus this ratio is an intrinsic property of the star, and you saw above that this ratio is related to the temperature of the star. The ratio is, of course, a measure of the relative amounts of two colors, and as such is called a *color index*. (Our experience of color is independent of both the brightness of the object and the distance to the object. It instead involves the *relative* amounts of the primary colors; hence the name for this ratio.) Any two wavelengths λ_1, λ_2 can be used to form such a color index, but clearly one should select wavelengths at which the stars are bright and $\lambda \lesssim \lambda_{max}$ (to avoid the Rayleigh-Jeans region where the ratio is independent of temperature).

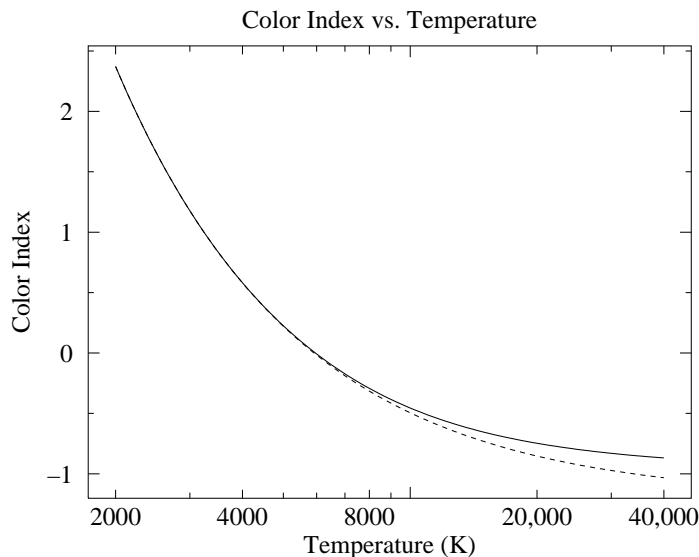[14]Do notice the absence of h in this classical result.

Color Index vs. Temperature

Figure 4.2: In the case where $\lambda_1 = .436 \; \mu$m (blue) and $\lambda_2 = .545 \; \mu$m (green or 'visible'), the 'color index' $2.5 \log(F_2/F_1)$ is plotted as a function of temperature. The dotted line shows the approximate result Eq. 4.10; the solid line shows the actual ratio of Planck functions. Do remember that high temperature stars have a smaller, even negative, color index.

Magnitude

For historical reasons, astronomers typically measure light in *magnitudes*. Magnitudes are related to fluxes by:

$$m = -2.5 \log_{10}(F/F_0) \tag{4.13}$$

where F_0 is the standardizing[15] flux that corresponds to $m = 0$. In astronomy log commonly[16] refers to $\log_{10}$ (and so in the rest of this chapter I now drop the $_{10}$), although we could equivalently write this equation in terms of other bases:

$$m = -2.5 \log_{10}(F/F_0) = -1.085736 \; \ln(F/F_0) = -\log_{2.511886}(F/F_0) \tag{4.14}$$

The minus sign in this definition means that magnitudes work backwards: the brighter the star, the *smaller* the magnitude. Very bright objects would have negative magnitudes. Since the measured flux of a star depends on distance, magnitude is not an intrinsic property of a star. Assuming transparent space, magnitude can be related to luminosity and distance:

$$m = -2.5 \log \left(\frac{L}{4\pi r^2 F_0} \right) \tag{4.15}$$

Thus if a star's luminosity is known and its magnitude measured, its distance can be calculated. Astronomers define the *absolute magnitude* of a star to be the magnitude the star

---

[15]Historically F_0 was defined as the flux of the star Vega, so Vega by definition had magnitude zero and color index zero.

[16]Pun intended. Use of $\log_{10}$ is a bit old fashion. If you see 'log' (without an explicit base or further comment) in a modern physics document, you should probably assume $\ln = \log_e$ is intended, unless something historical is being discussed (like stellar magnitudes, dB or pH).

would have if observed from a distance of 10 pc[17]. Thus:

$$m = -2.5 \log \left[\frac{L}{4\pi r^2 F_0} \right] \tag{4.16}$$

$$= -2.5 \log \left[\left(\frac{L}{4\pi (10 \text{ pc})^2 F_0} \right) \cdot \left(\frac{10 \text{ pc}}{r} \right)^2 \right] \tag{4.17}$$

$$= -2.5 \log \left[\frac{L}{4\pi (10 \text{ pc})^2 F_0} \right] + 5 \log \left[\frac{r}{10 \text{ pc}} \right] \tag{4.18}$$

$$= M + 5 \log \left[\frac{r}{10 \text{ pc}} \right] \tag{4.19}$$

where M is the absolute magnitude and the remaining term: $5 \log(r/10 \text{ pc})$ is known as the distance modulus. The main point here is that distance affects magnitude as a constant offset. This result is a lemma of the general result:

Theorem: If the measured flux F_m is a fraction (ϵ) of the actual flux F (as would occur due to a less-than-perfectly efficient detector, a dusty mirror, atmospheric absorption, absorption due to interstellar dust,...) the resulting magnitude as measured (m_m) is just a constant ($2.5 \log \epsilon$) off from the actual magnitude (m).

Proof:

$$m_m = -2.5 \log(F_m/F_0) \tag{4.20}$$

$$= -2.5 \log(\epsilon F/F_0) \tag{4.21}$$

$$= -2.5 \log(F/F_0) - 2.5 \log(\epsilon) \tag{4.22}$$

$$= m - 2.5 \log(\epsilon) \tag{4.23}$$

In order to calculate flux (W/m^2) from photon count rates, we must divide by the photon collection efficiency, multiply by the energy per photon and divide by the collecting area of the telescope. But why bother: the above theorem says these multiplicative factors just result in a constant offset between the correctly calculated magnitude and one that simply ignores these factors. Furthermore, many of these complicating factors (e.g., the fraction of photons absorbed in the atmosphere) cannot be known in advance. Since some of these factors cannot be known in advance, the plan is to ignore all of them (so the computer program[18] calculating magnitude will not ask you for the energy/photon, quantum efficiency, telescope aperture, etc.), and instead experimentally determine the offset between the computer's magnitudes (which we will denote in lowercase, e.g., b) and the standard magnitude (uppercase: B). So part of this lab will involve finding the constant offset that relates our measured (instrumental) magnitudes to the actual (standardized) magnitude.
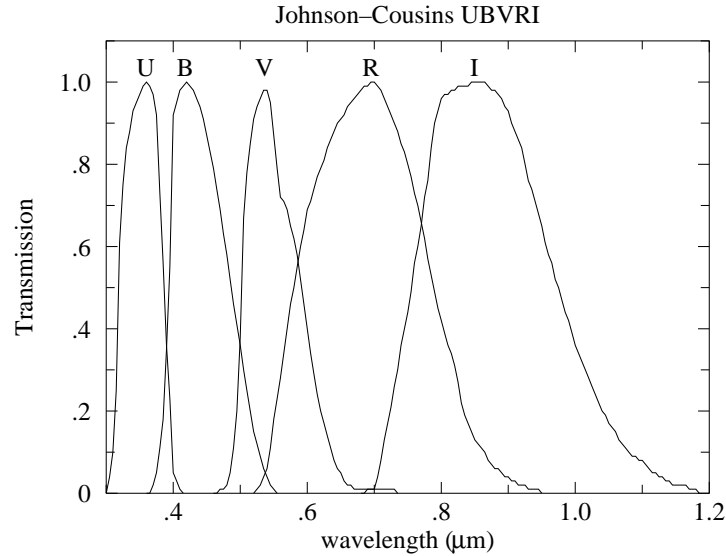
Filters

In the above equation for magnitude, the flux might be the total (all wavelengths or 'bolometric') light flux, or a monochromatic flux density F_λ, or the flux in a particular range of wavelengths. Much of astronomy is concerned with the flux through the five standard[19]

---

[17]pc = parsec = 3.0857×10^{16} m = 3.2616 Ly

[18]`gaia` magnitudes are calculated as: $50 - 2.5 \log(\text{gain} \times \text{net\_counts}/\text{exposure\_time})$

[19]Johnson, H. L. and Morgan, W. W. (1951) ApJ **114** 522 & (1953) ApJ **117** 313
Cousins, A.W.J. (1976) memRAS **81** 25

Figure 4.3: The characteristics of the standard filters: U (ultraviolet), B (blue), V (visible), R (red), I (infrared) from *Allen's Astrophysical Quantities* p. 387 and The General Catalogue of Photometric Data: `http://obswww.unige.ch/gcpd/system.html`

U, B, V, R, and I filters. The characteristics of these filters are detailed in Figure 4.3, but essentially each filter allows transmission of a range of wavelengths $\Delta\lambda$, centered on a particular wavelength. The name of the filter reports the type of light allowed to pass: U (ultraviolet), B (blue), V ('visible', actually green), R (red), and I (infrared). The filters are broad enough that the resulting bin really doesn't well represent a value for F_λ. (An appendix to this chapter describes the $u'g'r'i'z'$ filters[20] used in the Sloan Digital Sky Survey.)

The magnitude of a star as measured through a B filter is called the B magnitude and is simply denoted: B. Notice that we can now form color indices just by subtracting two magnitudes. For example, the most common color index is $B - V$:

$$B - V = 2.5\left(\log(F_V/F_{V0}) - \log(F_B/F_{B0})\right) \tag{4.24}$$

$$= 2.5\left(\log(F_V/F_B) + \log(F_{B0}/F_{V0})\right) \tag{4.25}$$

$$= 2.5\log(F_V/F_B) + \text{constant} \tag{4.26}$$

So $B - V$ is related to the flux ratio F_V/F_B and so is an intrinsic property of the star related to temperature. Furthermore, while Eq. 4.10 was derived assuming monochromatic

---

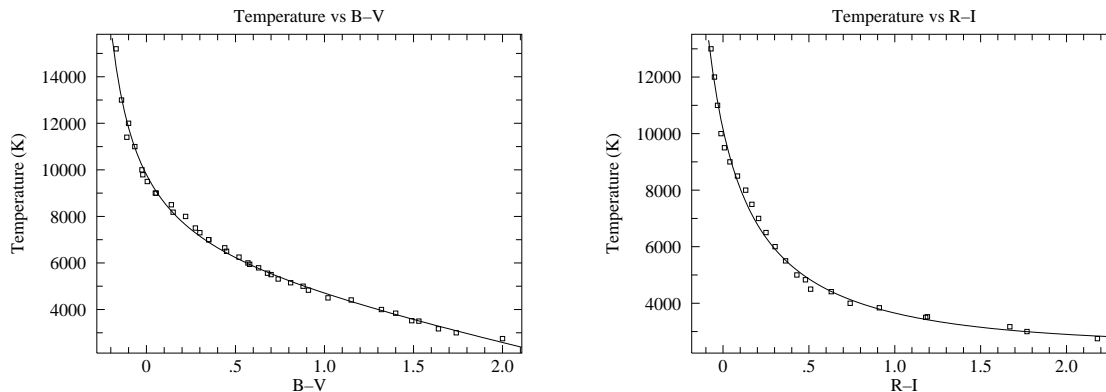[20]Fukugita, M., Ichikawa, T., Gunn, J. E., et al. 1996 AJ, 111, 1748

Figure 4.4: Using data from *Allen's Astrophysics Quantities* calibration curves relating stellar temperature to color index can be obtained. The fit equations for these curves is given in the text.

flux densities (in contrast to the broad band fluxes that make up B and V), we can still hope equations similar to Eq. 4.10 can be derived for $B - V$. *Allen's Astrophysical Quantities* provides calibration data to which Kirkman has fit a curve:

$$B - V = \frac{35800}{T + 3960} - 3.67 + 1.08 \times 10^{-4} \, T \tag{4.27}$$

and the inverse relationship:

$$T = \frac{1700}{(B - V) + .36} + 5060 - 1600(B - V) \tag{4.28}$$

The data with fitted curve is plotted in Figure 4.4. Notice that for $B - V < 0$ small uncertainties in $B - V$ result in large uncertainties in T: it would probably we wise to switch to a different color index like $U - B$ to measure the temperature of such a hot star.

Similar work can be done for $R - I$, with results:

$$T = \frac{2750}{(R - I) + .314} + 1400 + 160(R - I) \tag{4.29}$$

For the Sun, *Allen's Astrophysics Quantities* reports: T=5777 K, $B - V$=0.65, $R - I$=0.34 whereas Eq. 4.28 gives 5703 K and Eq. 4.29 gives 5659 K. In general errors of a few percent should be expected.

Temperature II

The starting point for physics is usually hard intrinsic quantities like temperature, density and pressure. However, in astronomy the transducers[21] used to measure these quantities are

---

[21] In normal usage, a transducer is a device which converts a physical quantity (e.g., pressure, temperature, force,...) to an electrical quantity (volts, amps, Hz ...) for convenient measurement: for example, a microphone. Here I've broadened the usual meaning to include natural 'devices' whose emitted or absorbed *light* allows a physical quantity to be determined. Obviously we are connected to the stars by light, not copper wires.

Telescope	Meade LX200		CCD	Kodak KAF-1001E
aperture	12"		pixel	24 μm $\times$ 24 μm
focal ratio	f/10		full-well	$\sim$ 150,000 e^-/pixel
focal length	120"		read noise	15 e^- rms
			gain	2.03 e^-/ADU
Filter Wheel	SBIG FW8-STL			
filters	blank, $BVRI$, $g'r'i'$		λ	Quantum Efficiency
Camera	SBIG ST-1001E NABG		.95 μm	20%
pixels	1024 $\times$ 1024		.80 μm	50%
image	28$'$ $\times$ 28$'$		.65 μm	65%
scale	1.65"/pixel		.50 μm	50%
weight	7.5 lbs		.35 μm	20%

Table 4.1: CCD photometry equipment used at the SJU observatory.

parts of the star itself (say the absorption lines of a particular element in the atmosphere of the star). We will always be a bit uncertain about the exact situation of these transducers, and hence the calibration of these transducers is correspondingly uncertain. For example stars with unusual chemical composition (like population II stars) or unusual surface gravity g (like giant stars) really deserve separate calibration curves. Since the usual physical quantities are in astronomy provisional and subject to recalibration, astronomers attach primary importance to the quantities that are not subject to the whims of revised theory: the actual measurements of light intensity. Thus astronomers use as much as possible hard quantities[22] like $B - V$ directly without converting them to temperature using some provisional formula. For example just using $B - V$, stars can be arranged in temperature-increasing order, since there is a monotone relationship between $B - V$ and T. Of course, in this lab the aim is to measure star temperatures in normal units.

Summary

In this lab you will measure the temperature of stars by measuring their B, V, R, I magnitudes, calculating the color indices $B-V$ and $R-I$, and then, using the supplied calibration curves, find T. The calibration curves are based on detailed spectra of bright, normal stars; In using these calibration curves we are automatically assuming our (distant and hence dimmer) target stars are also 'normal'.

Detector System

In this lab photons are counted using a *charge coupled device* or CCD. Our Kodak KAF-1001E CCD consists of a typical 26-pin DIP integrated circuit with a window that exposes to

---

[22]In this lab you will see that even as simple a quantity as B is actually only distantly related to direct meter readings. The direct meter readings must be 'reduced' to eliminate confounding factors like detector efficiency or atmospheric absorption. Nevertheless, since these problems are 'at hand' astronomers believe that they can be properly treated. Astronomers willing archive B data, whereas T calculations are always considered provisional.

light a 1"×1" field of 1024×1024 light sensitive regions or pixels. Photons incident on a pixel free electrons via the photoelectric effect[23]. Each pixel stores its charge during an exposure, and then each bucket of charge is transferred (in a manner similar to a bucket brigade) to a capacitor where it produces a voltage proportional to the number of electrons. An analog-to-digital converter then converts that voltage to a 16-bit binary number (decimal: 0–65535). A CCD image is thus a 1024×1024 matrix of integers. The units of these integers is simply ADU for analog to digital units, but ideally the result should be proportional to the number of incident photons. The combined effects of photon$\rightarrow e^-$ efficiency ('quantum efficiency') and $e^- \rightarrow$ ADU ('gain') means that there are ~ 4 times as many incident photons as ADU counts. Electron storage in a pixel is limited to a full-well capacity of $\sim 150,000\ e^-$; additional photoelectrons will simply leak out of the well.

The Kodak CCD is contained within (and controlled by) a STL-1001E camera made by the Santa Barbara Instrument Group[24]. In front of the camera, an SBIG FW8-STL filter wheel allows computer controlled placement of one of the B, V, R, I, g', r', i' filters or a blank.

The SBIG camera is mounted on a Meade 12" LX200 Schmidt-Cassegrain Catadioptric telescope. The orientation of the telescope is controlled by a Paramount ME mount using TheSkyX[25] software. Once the telescope has been initialized the telescope control software allows the telescope to be directed to a long list of cataloged objects or to any location specified by RA/dec[26].

Linearity

In an ideal CCD, the count in a particular pixel should be proportional to the number of photons absorbed, which in turn should be proportional to the exposure time. This proportionality fails for large exposures and the CCD saturates as the count approaches 60,000 ADU. (The count actually jumps *up* to the 16-bit maximum 65535 on saturation.) Of course, if a pixel is saturated, additional photons are missed, and the (now pegged) ADU count falls below actual photon flux. CCD linearity was tested by varying the exposure time. The results are displayed in Figure 4.5.

The calculated magnitude of a star—a measurement of the photon flux (counts/time)—should not depend on the exposure time. Of course, for very short exposures the handful of counts above background is subject to a relatively large random fluctuation, and so the magnitude will have a relatively large uncertainty. As we've just learned, sufficiently long exposures will result in pixel saturation and hence a systematically low count and a too-large (dim) magnitude. As shown in Figure 4.6, there is a large range of exposures (including those with slight saturation) which can produce an accurate magnitude.

---

[23]Albert Einstein (1879–1955) received the 1921 Nobel prize for his 1905 theory explaining this effect. Robert Millikan's [(1868–1953), B.A. Oberlin College, Ph.D. Columbia] experimental studies (1912–1915) of the photoelectric effect were cited, in part, for his Nobel in 1923.

[24]`www.sbig.com`

[25]both from `bisque.com`

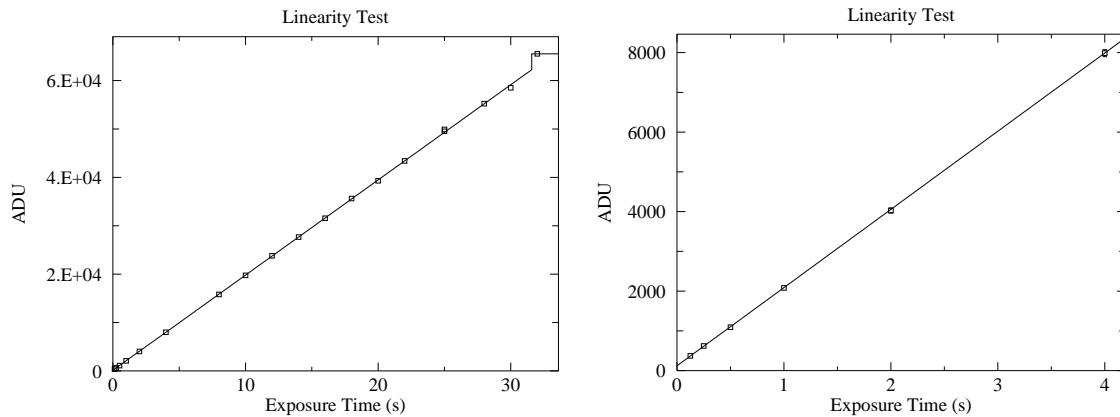[26]See page 85 for a list of online tutorials covering basic astronomy vocabulary.

Figure 4.5: Below $\sim 60,000$ ADU (30 second exposure) the response of our CCD seems to be linear (reduced $\chi^2 \sim 1$ for errors approximated as $\sqrt{\text{ADU}}$—generally an overestimate for error), with saturation evident in the 32 second exposure. (At $\sim 62,000$ ADU the count jumps up to the 16-bit maximum 65535.) The linear fit even looks good at minimum exposure times where systematic error in the shutter speed control is expected. Note that the y intercept is not exactly zero: with this camera zero-time exposures are designed to produce an output of about 100 ADU.
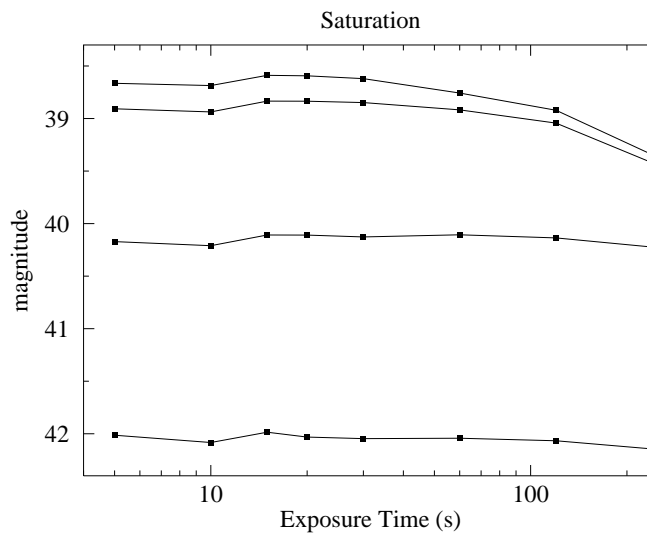

Figure 4.6: The magnitude of four stars was calculated from frames with various exposures. The brightest two stars have saturated pixels in 20 sec exposures and the dimming magnitude is evident in exposures longer than 30 sec. The third brightest star begins to be saturated at 240 sec. The fourth star is not saturated. Notice that a handful of saturated pixels will generally not result in a large magnitude error.

Flat Frame

Individual pixels have different sensitivities to light. While the effect is not large ($\sim 5\%$), it would be a leading source of uncertainty if not corrected. The solution is (in theory) simple: take a picture of a uniformly illuminated surface, and record the count in each pixel. Evidently this 'flat frame' count records how each pixel responds to one particular flux level. If in another frame a pixel records some fraction of its flat-frame count, linearity guarantees that the measured flux level is that same fraction of the flat-frame flux level. Thus to correct for varying sensitivities we just divide (pixel by pixel) the raw CCD frame by the flat frame.

In practice it is difficult to obtain a uniformly illuminated surface. In a *sky flat*, one assumes that the small section of a blue sky covered in a CCD frame is uniform. (Typically this is done after sunset so the sky is dim enough to avoid saturation in the short ($\lesssim 1$ sec) exposure, but not so dim that stars show through.) In a *dome flat* we attempt to uniformly illuminate a white surface with electric lights. Whatever the source of the flat, it is best to average several of them to average out non-uniformities in the source.

It should be clear that a flat frame records the *overall* efficiency of the system: both the varying quantum efficiency of individual pixels and the ability of the telescope to gather light and concentrate it on a particular pixel. Generally the optical efficiency of a telescope decreases for sources far from the optical axis. The off-axis limits (where the optical efficiency approaches zero) define a telescope's maximum field-of-view. The limited optical efficiency near the edge of the field of view leads to 'vignetting': the gradual fade of optical efficiency to zero at the extreme edge. In addition optical flaws, like dust on optical surfaces, are recorded in a flat frame. As a result a flat frame depends on the entire detection system (telescope, filter, chip) and will gradually change, as for example, dust accumulates on the mirror.

Bias Frame

A careful examination of the linearity plots in Figure 4.5, shows that they do not go through the origin. That is, a zero-time[27] exposure produces some counts, simply by the process of reading the CCD. The uncertainty in this bias frame (the 'read noise') represents the minimum background noise in any pixel. Measurements on our CCD shows that the difference between two bias frames shows an approximately normal distribution (aside from the flaws) with a standard deviation ~ 11 ADU. Also note that the system artificially introduces an offset of 100 into each pixel, so $\frac{2}{3}$ of the pixels in a single bias frame are expected in the range 100 ± 8 ADU. ($8 \approx 11/\sqrt{2}$)

Dark Frame

Even in the total absence of light, pixels will slowly accumulate charge. The electric current leaking into the pixels is strongly affected by temperature, hence the name 'thermal current' and it produces accumulated charge in the absence of starlight, hence the name 'dark current'. The professional solution is to cool the CCD using liquid nitrogen, which

---

[27]With the STL-1001E the minimum exposure is actually 0.12 s
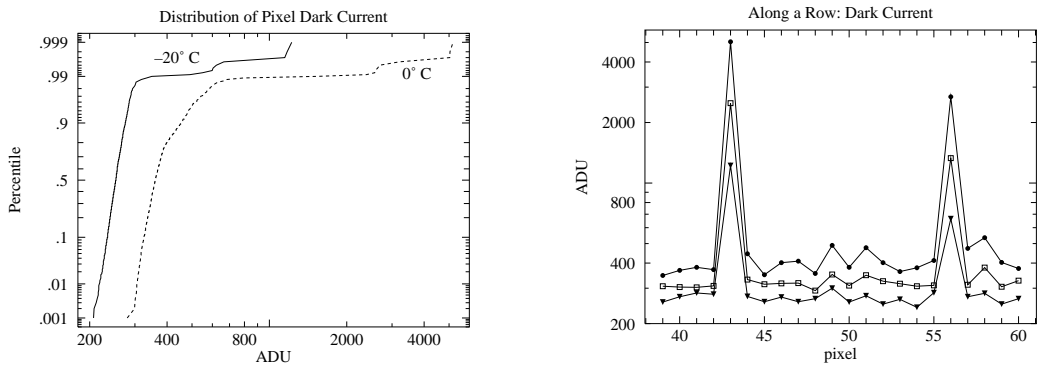
(a) The distribution of pixel dark current at $0°C$ and $-20°C$. All but a few of the pixels have a (log)normal distribution of dark current. About 1% percent of the pixels show much larger dark current: these are the 'hot' pixels. Note that both classes of pixels respond to temperature: lowering the temperature reduces every pixel's dark current.

(b) Part of a row of pixels is displayed at three temperatures: ● = $0°C$, □ = $-10°C$, ▼ = $-20°C$. Isolated hot pixels are randomly sprinkled throughout the image (here at columns 43 and 56). The data here and in (a) are from 15 minute dark frames.
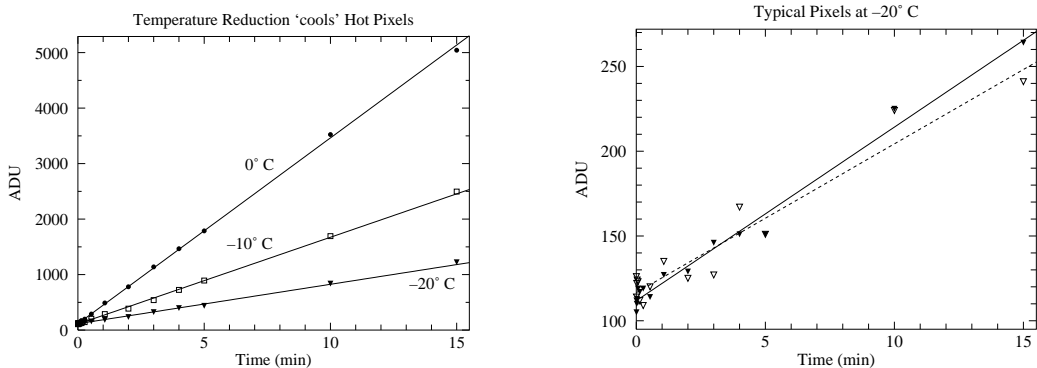
(c) Pixel counts grow with 'exposure' time as the dark current produces ever larger stored charge in a pixel; of course reducing the temperature reduces the dark current.

(d) While it is more evident in this low count data, there is always random deviation in counts. While we can subtract the average dark charge, deviations from the average produce 'noise' in our images. Reducing the temperature reduces this noise.

Figure 4.7: Dark frames are 'exposures' with the shutter closed. The source of these counts is not starlight, rather a thermally induced current allows charge to accumulate in each pixel. This 'dark current' can be exceptionally large in 'hot pixels'.

reduces the dark currents to near zero. The STL-1001E uses a less cumbersome (but less effective) solution: a thermoelectric cooler which can cool the CCD $\sim 40°$C below ambient temperature, reducing the dark currents by more than a factor of 10. The resulting dark currents are *not* negligible for exposures longer than a few minutes. A 'dark frame' is simply an 'exposure' with the shutter closed; it is a bias frame plus accumulated charge due to dark currents. A dark frame can be subtracted from an (equally timed) exposed frame to compensate for this non-photon-induced current, however variation in the dark current ('noise') results in a corresponding uncertainty in the adjusted pixel counts.

There is tremendous pixel-to-pixel variation in the dark current. About 1% of the pixels have a dark currents ~ 10 times the typical value. The 'hottest' pixels[28] will saturate in a 5 minute exposure at $0°$C. Thus a dark frame looks black except for a handful of bright ('hot') pixels; it could be mistaken for the night sky, except the 'stars' are not bright disks rather isolated, single hot pixels. Since taking a dark frame takes as much time as a real exposure, use dark frames only when required: when you are taking real data. Simply learn to disregard the sprinkling of isolated hot pixels in non data-taking situations.

Since the dark current depends on temperature, the CCD needs to achieve a stable temperature before the dark frames are taken. The CCD has an on-board thermometer, but a stable temperature at one point does not mean that the temperature as stabilized throughout the CCD. Direct measures displayed in Figure 4.8 show that it may take several hours to achieve reproducible dark frames. And the lower the requested temperature the longer it takes to achieve thermal equilibrium. For a requested temperature of $-20°$C, 1.8 hours are required for 95% (e^{-3} with $\tau \approx 0.6$ hour) of the excess counts to be eliminated. For a requested temperature of $-10°$C, 0.8 hours are required for 95% (e^{-3} with $\tau \approx 0.26$ hour) of the excess counts to be eliminated. When requesting particularly low CCD temperatures it is advisable to take dark frames at the end of the observing session or to cool down the camera well before sunset. (That is, the obvious time time to take dark frames—at dust between taking sky flats and dark-sky frames—may not be the best time to take the dark frames.)

Data Frames

The term 'object frame' here refers to a raw CCD frame of the sky as delivered by the camera-controlling software. If the object frame was not automatically dark-subtracted, there must be a matching (time & temperature) dark frame. A 'reduced frame' is an object frame that has been dark-subtracted and flat-field corrected. By adjusting for non-photon-induced charge and varying pixel sensitivity, we hope our reduced frame shows the actual distribution of photons. It should be noted that all of these corrections will be applied by making the proper requests of the CCD control software. In the end, you should retain both the fully processed reduced frame and the original object frame.

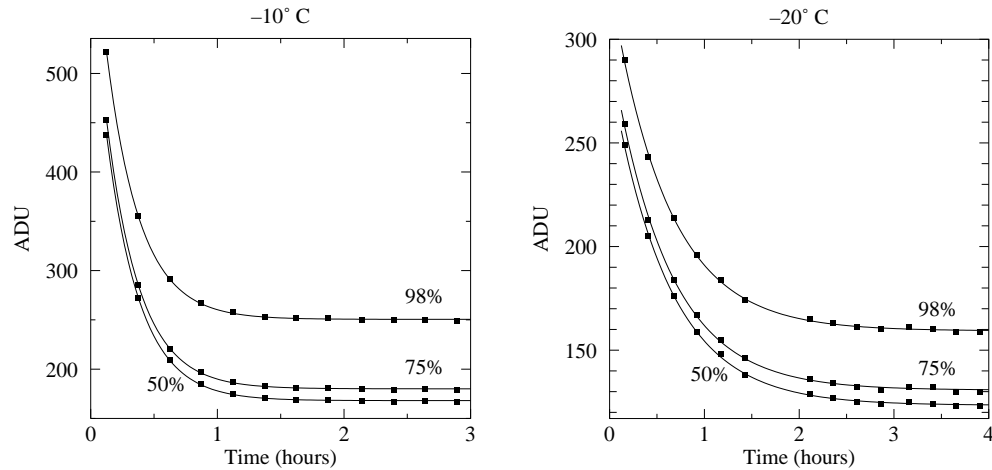[28]For example: $(265, 742), (68, 97), (233, 866), (266, 166)$

Figure 4.8: It can take hours to achieve a stable CCD temperature. The left plot displays the results of a sequence of 900 sec dark frames at an indicated (stable) temperature of $-10°$C. The count for the median (50 percentile), 75%, and 98% pixel is displayed as a function of time. In all cases the approach to equilibrium is exponential with $\tau \approx 0.26$ hours. Analogous results for $-20°$C show a much slower approach to equilibrium ($\tau \approx 0.8$ hours).

Basic Plan

Given a reduced frame, determining the number of counts/second from a star is a relatively straightforward[29] task which will be performed (with your help) by the software. This resulting rate must be converted to flux by multiplying (or dividing) by a variety of factors: collecting area of the telescope, reflectivity of the mirror, quantum efficiency of the CCD, CCD gain, ... However the main point is that there is a proportionality between this rate and the actual flux. By our theorem, this means that a magnitude calculated just using this rate (an 'instrumental magnitude') is just a constant off from the actual standardized magnitude. If we have a star in the reduced frame of known magnitude, that constant difference can be calculated just by taking the difference between the instrumental magnitude and the known magnitude. And then that calibrating constant can be applied to every star in the reduced frame, converting each instrumental magnitude to a standardized magnitude. In practice it is wise to use several calibrating stars and use the average value of magnitude difference as the calibration constant. (The standard deviation of the magnitude differences then gives us an estimate for the error.) The calculation of instrumental magnitudes (i.e., calculating $-2.5 \log(\text{rate})$) is also a straightforward task best left to software. All you will need to do is calculate (probably using a spreadsheet) the magnitude differences of the calibrating stars, and then find their mean and standard deviation.

---

[29]Many important details are hereby hidden from view. A short list: (1) determining the background level to be subtracted from the star pixels (2) determining the proper aperture that encloses all the stars light or accounting for the star's light that has blended into the background (3) accounting for the star's light that is between pixels (4) dealing with pixels that are only fractionally within the aperture. In summary: background and point spread function (PSF) are the key issues.
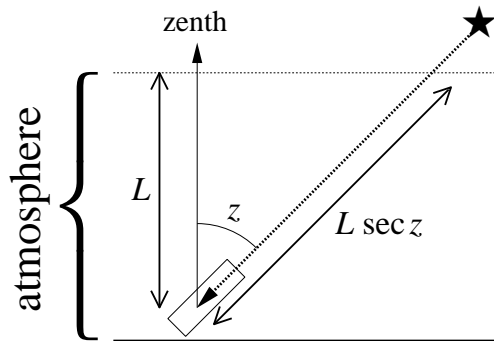
Figure 4.9: Stars that are near zenith go through the minimum amount of the Earth's atmosphere. Stars at a zenith angle z go through $\sec z$ times that minimum. This figure displays the atmosphere as a finite thickness slab, whereas in fact the atmosphere gradually thins out to nothing. Nevertheless, meter-by-meter a star at angle z must go through $\sec z$ times as much atmosphere as a star at zenith. 'Air mass' is defined as this multiplicative factor: $\sec z$.

Complications

Air Mass Corrections

Magnitudes are intended to be archivable numbers in which the particulars of the observation (e.g., telescope aperture, quantum efficiency, transparency of the atmosphere,...) have been removed. As describe above, this is relatively easy if the reduced frame contains calibrated sources. On the other hand, if we have separate reduced frames for the object and calibrated stars, we must arrange that the entire detection system (atmosphere included) acts the same (i.e., the same proportionality constant between rate and flux) for both frames. However, it is difficult to find calibrated stars that have the same angular altitude as the object; Thus one frame must be shot through a thicker slice of atmospheric than the other. Air mass corrections adjust for this path length difference and assume that the atmospheres (and optics) were otherwise identical.

The absorption of light is a multiplicative phenomenon; that is, if the first meter of the atmosphere allows fractional transmission of light T_1 and the next T_2, etc, then the intensity of light through a sequence of meters is:

$$F = T_N T_{N-1} \cdots T_2 T_1 \, F_0 = \prod_{i=1}^{N} T_i \, F_0 \tag{4.30}$$

Since it is easier to deal with additive quantities rather than multiplicative quantities we define the optical depth τ by:

$$T \equiv e^{-\tau} \tag{4.31}$$

so

$$F = T_N T_{N-1} \cdots T_2 T_1 \, F_0 = \exp\left(-\sum_{i=1}^{N} \tau_i\right) F_0 \tag{4.32}$$

According the Beer-Lambert law, the absorption of light depends on atomic absorptivity (the 'cross section' σ, which generally depends on the wavelength of light), the number of atoms per volume ('number density' n), and the path length ℓ:

$$\tau = \sigma n \ell \tag{4.33}$$

We can think of the atmosphere as a sequence of filters, so the light intensity through the atmosphere is:

$$F = \exp\left(-\sum_{i=1}^{N} \sigma n \Delta \ell\right) F_0 = \exp\left(-\int \sigma n \, d\ell\right) F_0 \tag{4.34}$$

Of course the density of the atmosphere (and to some extent the composition of the atmosphere) depends on altitude. If we consider light that has taken the shortest path through the atmosphere (i.e., from a star directly overhead or at *zenith*), we call the above integral $\tau_0(\lambda)$. (The dependence of τ_0 on the wavelength of light is of course due to the dependence of σ on the wavelength of light.) As shown in Figure 4.9, if a star is at zenith angle z, the path length (and hence τ) in increased by the *air mass* factor $\sec z$. Thus:

$$F = \exp\left(-\tau_0 \ \sec z\right) F_0 \tag{4.35}$$

The magnitude that corresponds to this flux is:

$$m = 2.5\tau_0 \log e \ \sec z + m_0 \tag{4.36}$$

where m is the magnitude measured at zenith angle z and m_0 is the magnitude as measured without any atmospheric absorption (i.e., the standardized magnitude). For any single star one can (assuming the atmosphere doesn't change over the few hours required) plot $(\sec z, m)$ data as the star rises, culminates and sets, and determine the y-intercept which is m_0. Alternatively for a set of stars each with known m_0 and measured m at varying $\sec z$, one can determine the correction factors A and B required to convert a star's $(\sec z, m)$ to m_0:

$$m - m_0 = B \sec z + A \tag{4.37}$$

Thus lacking in-frame calibrated stars, several calibration frames (at different $\sec z$) are required for each filter, and the reduction process becomes much more complicated.

Note that the zenith angle z can be calculated[30] from:

$$\cos z = \sin \delta \sin \varphi + \cos \delta \cos h \cos \varphi \tag{4.38}$$

where δ and h are the star's declination and hour angle and φ is the observatory's latitude. The above terms from astrometry (declination, hour angle, altitude, zenith, right ascension, . . .) are part of the everyday vocabulary of astronomers. If you are not familiar with these terms you should read the following online tutorials:

- `http://www.physics.csbsju.edu/astro/CS/CSintro.html`

- `http://www.physics.csbsju.edu/astro/sky/sky.01.html`

- `http://www.physics.csbsju.edu/astro/terms.html`

For example at SJU ($\varphi = 45°34.5'$) for stars on the celestial equator ($\delta = 0$), the minimum air mass (at $h = 0^h$) is $\sec z = 1.43$. The sequence of air masses: $\sec z$=1.5, 2.0, 2.5, 3.0 occurs at hour angles $h = \pm 1.18^h, \pm 2.96^h, \pm 3.68^h, \pm 4.10^h$. Figure 4.11 plots these air mass values for other declinations.
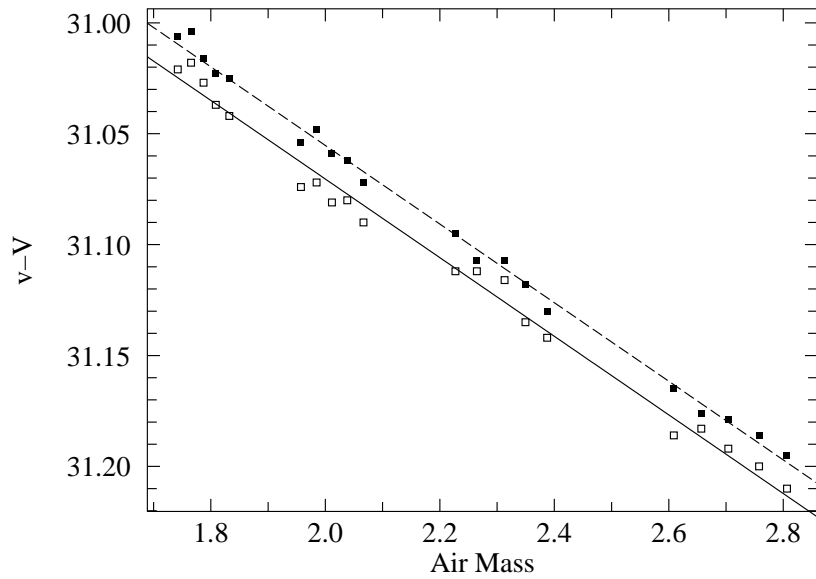
---

[30]`xephem` can do this calculation for you

Figure 4.10: The instrumental magnitude minus the standardized magnitude $(v - V)$ for a red star ($\square$) and a blue star ($\blacksquare$) as a function of the air mass. Notice that the slopes are quite similar (i.e., $.177 \sec z$), but the intercepts are slightly different ($\Delta = 0.016(B - V)$), due to the difference in color. This color correction is explained in the following section. The rms deviation in these fits is 0.005 magnitudes which is about $\frac{1}{3}$ the intercept shift.
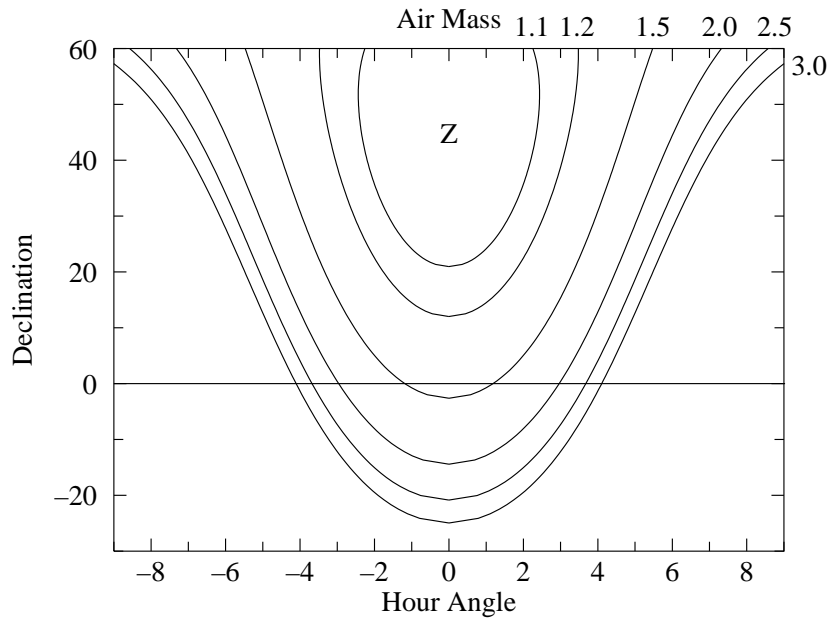

Figure 4.11: Air mass ($\sec z$) depends on where a star is in the sky. Air mass is plotted here as a function of the star's declination and hour angle for the SJU observatory location. Z marks zenith, where the minimum (1) air mass is found.
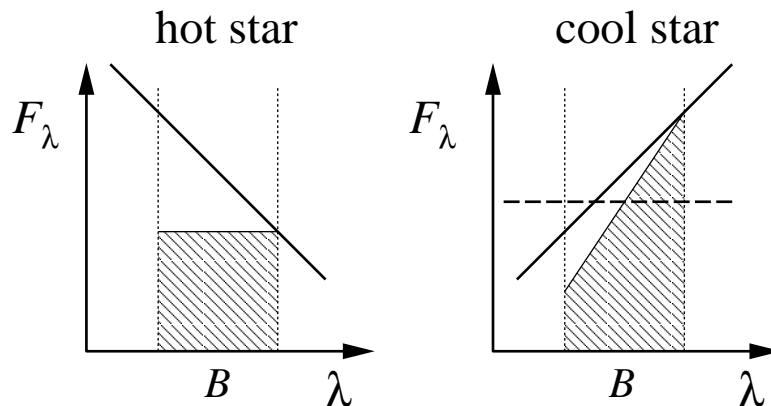
Figure 4.12: The atmosphere (in fact any optical component) acts as a colored filter on incident starlight. Typically short wavelength light is more strongly attenuated (i.e., reduced) than long wavelength light. Consider two stars that have the same B magnitude outside the atmosphere. Of course, the hot star has a larger fraction of its light in the short wavelength side of the B band. As a result more of its light will be affected and its measured magnitude will deviate from that of the cool star. In a tremendous exaggeration I've assumed above 50% absorption at the short-λ end of the B band, and 0% absorption at the long-λ end. As a result the total measured B-band flux (the shaded area) will be larger for the cool star even though both stars had the same flux outside the atmosphere. If narrow band filters are used there will be much less change in absorption over the band and so this effect is much reduced.

Color Corrections

We learned in the above section that the Earth's atmosphere acts as a non-negligible filter, attenuating (absorbing or scattering, generally reducing) starlight before it reaches our telescope. The fact that the atmosphere looks blue tells us that the atmosphere in fact acts as a colored filter, attenuating some wavelengths more than others. (That is, σ depends on λ, with short-λ (blue) light more attenuated than long-λ (red).) As discussed in Figure 4.12, this means that two stars which, outside our atmosphere have the same magnitude but different temperatures, will be measured as having different magnitudes from the ground. The upshot of this is the atmospheric optical depth parameter τ_0, depends (slightly) on the temperature, T, of the star:

$$B = 2.5 \ \tau_0(T) \ \log e \ \sec z + B_0 \tag{4.39}$$

where B is the magnitude through the B filter at ground level and B_0 is the atmosphere-free B magnitude. The temperature of the star is related to the actual $B_0 - V_0$ color index, which in turn is related to the instrumental color index $b - v$. If we make a first order Taylor expansion of $\tau_0(T)$ in terms of $b - v$, we have (after lumping together all the unknown constants and assuming all the stars in the frame have the same z)

$$b \approx \alpha_B + \beta_B(b - v) + B_0 \tag{4.40}$$

That is the offset between the instrumental magnitude and the atmosphere-free magnitude is not exactly a constant; instead we expect a slight dependence on the color of the star. A
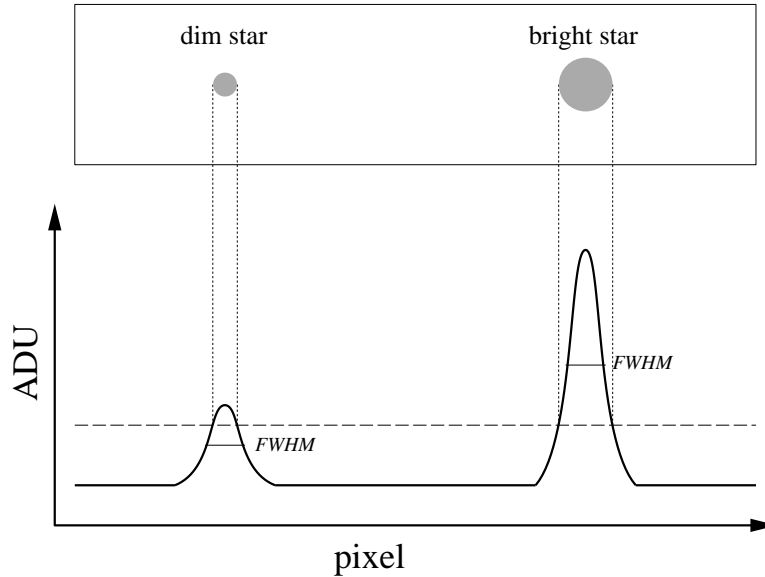
Figure 4.13: Every photon detected in a CCD frame has traversed (essentially) the same patch of atmosphere, so each star's image suffers the same distortion. Every stellar 'image' (really point spread function or PSF) has the same shape, only the total flux in each image varies (with the star's magnitude). However, a brief inspection of an image will show clearly larger spots for brighter stars. As shown above this is simply a matter of the level chosen as bright.

linear fit (using the data from the calibrated sources) can then be used to determine α and β, viz:

$$b - B_0 = \alpha_B + \beta_B(b - v) \tag{4.41}$$

and similarly for the V magnitudes:

$$v - V_0 = \alpha_V + \beta_V(b - v) \tag{4.42}$$

Subtracting these two equations gives us the relationship between the instrumental color index and the atmosphere-free color index:

$$(b - v) - (B_0 - V_0) = \alpha_B - \alpha_V + (\beta_B - \beta_V)(b - v) \tag{4.43}$$
$$[1 + (\beta_V - \beta_B)](b - v) + (\alpha_V - \alpha_B) = B_0 - V_0 \tag{4.44}$$

Thus we expect a linear relationship (with a nearly unit slope) between the instrumental color index and the atmosphere-free color index. The parameters of this linear relationship can be determined by a fit using the data from the calibrated stars.

Aperture Corrections

When you look at your CCD frames, you will not believe my statement that all the star images (really PSF) have the same size. However, both bright stars and dim stars are far enough away that their angular diameters are effectively zero (less than a thousandth of a single pixel). The photons from each star shoot through the Earth's atmosphere and are

deflected this way and that producing a multi-pixel disk in the frame. This is called atmospheric *seeing* (particularly for image size) or *scintillation* (particularly for image brightness). But since every photon is shot (basically) through the same patch of atmosphere, these random deflections must have the same distribution. The difference between a dim star and a bright star is simply the total number of photons in the images. (That is a long time exposure of a dim star should look exactly[31] like a short exposure of a bright star if the two cases produce the same number of photons.) To see that the distributions are identical you should look at the full width at half maximum (FWHM) of the PSF: First determine the peak count in an image, and then find the circle at which the count is half of this maximum. The diameter of the circle (typically a few arcsec) is the FWHM.

Because of the obvious difference in the image size, when totaling the counts in a stellar image, one is tempted to expand or reduce the circle of pixels counted as part of a star to match the apparent size of that star. *Do not do this!* Instead keep a constant aperture size for all frames. It may appear that counts will be missed as bright stars overflow the aperture, whereas dim stars have a too-large aperture. However recall that all stars actually have the same extent. Furthermore our theorem states that if we capture a consistent fraction of the counts in every star, all our instrumental magnitudes will just be a constant off from the standardized magnitudes. So a *consistent* fraction of the counts may be combined with all the other proportionality constants in the final difference between instrumental magnitude and standardized magnitude. Now there may be occasions where we must adjust the *aperture* used for magnitude calculation (for example to exclude a neighboring star), however then inconsistencies (and hence errors) are then being generated. The disadvantage of using a constant aperture is relatively more noise-prone 'background' pixels will be included in dim stars. There are a variety of solutions to this problems (generally under the heading of PSF fitting), however they are beyond the aims of this lab.

The blurring of star images (i.e., PSF) depends both on atmospheric seeing and the adjustment of the telescope. Clearly an out-of-focus telescope (see below) will distribute the same photons in a larger radius disk. It should also be noted that the telescope's 'optical aberrations' result in additional blurring ('coma') near the edge of the telescope's field of view.

Focus

The aim of focus is to achieve that smallest possible FWHM, so each star's light is concentrated in the fewest possible number of pixels. Same number of photons in fewer pixels, means a higher count in those central pixels. Since every pixel comes with a certain background 'noise', fewer pixels means less noise in the stellar magnitude. You should plan on spending a good bit of time (maybe a half hour) trying to achieve the best possible focus. There are two approaches to monitoring improved focus: (1) monitor the peak count in a bright star (~ 4 mag), (2) watch for the appearance of numerous dim stars as their peak gets above the 'bright' level. (You must learn to ignore the apparent size of bright stars: it is a poor measure of good focus.) A complicating factor is that both (1) and (2) vary independently of focus adjustments since atmospheric seeing varies from second to second, and since photon counts should be expected to vary $\sim \sqrt{N}$.

---

[31]We are assuming, of course, that the atmosphere acts the same during the long exposure as it does during the short exposure. No surprise: in fact the atmosphere is not time-invariant.

Software

xephem

`xephem` is planetarium software designed to display various types of night-sky maps in advance of observing. You will also use it to tabulate astrometry data relevant to your observations. The file `using.xephem.txt` describes how to use this program to produce the tables and maps required for the pre-observation phase of the lab. In addition you can use it for astrometry and photometry on `.fit` images (although I recommend `gaia` below for these reductions).

Aladin

`Aladin` is a front-end to various astronomy databases on the internet. You will use it to find images to use as finder maps and to identify (and obtain data on) the stars in those images. The Aladin server and SkyView+ are often a good sources of DSS (Digital Sky Survey using visible-light) images; Simbad[32] is the usual source for stellar information. Sometimes just information from the SAO catalog is required; then VizieR[33] can be used to access just the SAO catalog. You will use `Aladin` mostly in the pre-observation phase. The file `using.Aladin.txt` briefly describes how to use this program to produce the maps and data required for the pre-observation phase of the lab. Note: NASA has a very handy web page[34] that also allows you to do many of these things. `gaia` (see below) is also and excellent way to make finder maps.

CCDops

CCDOps is software used to control the camera and create/save CCD frames. You will be using a small fraction of its capabilities. Typical commands will be: to set the temperature (cooling) of the CCD, focus, grab images (set the exposure time and perhaps take a dark frame), examine images (histogram, crosshair), save images (in `.fit` and other formats), and reduce images by dark-subtracting, flat-fielding or averaging.

gaia

`gaia` is the recommended reduced-frame analysis program. In order to use `gaia` your images must be in either `.fit` or ndf (`.sdf`) format; you should use `.fit`. The file `using.gaia.txt` briefly describes how to use this program.

In addition to reporting a star's magnitude, `gaia` will report the error in that magnitude. This error is based on counting (Poisson statistics, $\sqrt{N}$). These errors will be smaller for brighter stars; a typical value might be ~ 0.003. Record one typical `gaia`-reported error

---

[32] `http://simbad.u-strasbg.fr/`

[33] `http://vizier.u-strasbg.fr/`

[34] `http://skyview.gsfc.nasa.gov/`: start with 1000×1000 pixel Digitized Sky Survey image with 0.5° Image Size, B-W Log Inverse Color Table, and a Grid

for your stars. Because of systematic errors, you will find the actual error is much larger ~ 0.02.

IRAF

`IRAF` is the Image Reduction and Analysis Facility, a general purpose software system for the reduction and analysis of astronomical data. It is the standard for professional astronomers: designed for the expert user—with no compromises for the beginner. While its use is encouraged for those thinking of becoming astronomers, I cannot recommend it for this lab. `ds9` (whose name really does derive from Star Trek) is an image viewer/creator that is often used in conjunction with IRAF.

Planning to Observe

Minnesota weather is is unpredictable[35] and we need an extraordinary, no-visible-clouds night. We must be prepared to use any/every of these rare nights on short notice. Of course, you have other commitments (your concert, the night before your math/physics exam, the St. Thomas game...), the aim here is to examine those constraints in well in advance and sign up only for dates you can guarantee attendance. Note that Murphy's Law guarantees that if you forget to X-out some important night (your girlfriend's birthday, the day before your term paper is due, a 'free' day), that night will be clear, and somebody (I hope not me!) is going to be disappointed. Intro astro labs are going X-out many Monday and Wednesday nights.

Mark on the class calendar (in PE132) the dates you and your lab partner(s) are committed to observe. In the afternoon of any day you've signed up for, contact me to confirm that the observatory is ready and that all involved know, not just the plan, but also the contingency plan (e.g., how/when I'll decide if the weather actually is a 'go').

Since clear nights are precious, 'go' days need a well-thought-out plan. If you're following the standard project, your plan involves a target whose frame will include several stars with known[36] B, V, R, I magnitudes. In the Fall this is often IC 4665 (a name that is known to `xephem`, `Aladin`, skyview, etc.). Thus you need to: (A) Find a target that has the required stars. (Stars with recorded R magnitudes are relatively rare.) (B) Know where those standard stars are in your target (so you can aim so your CCD frames to include the stars you need). (C) Know where your target is among the neighboring stars (so if your first try at finding the target fails, you have a plan [not 'hunt-and-peck'] for getting to the right spot). (D) And of course, know that your target is well above the horizon when you are planning to observe. While the standard project does not require additional standard stars, you may want you to record alternative (out-of-frame) standards.

---

[35]`http://www.physics.csbsju.edu/astro/` has a link designed to report (guess) sky conditions at the SJU observatory. It cannot be relied on, but I believe it's the best available information. Note: black is good for this clear sky clock.

[36]Professionally, only very carefully measured 'standard' stars—for example those measured by Landolt or Stetson—would be used for calibration. For the purposes of this lab you may use any star that has a 'book' magnitude. It is not at all unusual for such literature magnitudes to have 10% errors

Pre-observation Checklist

From the class web site find `photometry/observatoryCCD4.txt`. Print out a copy. You will cut out and tape relevant sections of this file as part of your lab notebook Procedure. Of course you will annotate this outline procedure so you have a record of exactly how your ran the telescopes (particularly the procedure to control the software).

The following should be prepared for one of your candidate observing dates:

1. Sunset time. (Typically you are expected to arrive at the observatory $\sim$30 minutes before sunset.)

2. Using `xephem` set for about two hours after sunset print out the following:

   (a) A Sky View showing the entire sky with the labeled location of the target.
   (b) A `.xephem/datatbl.txt` file recording basic data (RA, dec, altitude, air mass, ...) for the target at the suggested observation time. The file `using.xephem.txt` describes what data you need to have recorded.

3. Using `Aladin` (or web-based `skyview.gsfc.nasa.gov`) print out the following finding charts for your target cluster:

   (a) a low magnification (degree scale) image showing the desired CCD frame.
   (b) an image scaled to about the CCD frame size ($0.5°$) showing exactly the desired CCD frame. (Since the target CCD frame must include calibrated stars, clearly you must know where the calibrated stars are in the target.) Record the RA and dec for your target frame(s).

Learning to effectively use these pre-observation programs will be a bit of a challenge and take several hours, so do not procrastinate and feel free to seek my help. In addition to the usual problems of learning new software, you will need to learn how to make the web-based astronomy databases find the information you need. However, if you've failed to make these pre-observation finding charts, you can probably still make observations using one of the perennial targets (IC 4665 in the fall, M 67 in the spring).

Observation Evening

In order to take data the sky needs to be 90% cloud free: we must be able to aim the telescope at a star and not have a cloud go through that spot for an hour. Years of experience shows it is not possible to predict, even an hour before sunset, what the sky will be like at sunset. Thus the plan is for you to look at the sky 45–30 minutes before sunset and decide if the sky is suitable. Kirkman will do the same, and if we both reach the same conclusion (not a sure outcome!) we will both arrive at the observatory 30 minutes before sunset. Since we need to take flats during sunset, if all parties don't arrive well before sunset, the observing session is canceled. Plan to be at the observatory for 2–3 hours (no eating in the observatory; no bathroom in the observatory). Perhaps an hour of that period (after flats, waiting for the sky to darken) will involve really monotonous tasks: feel free to bring homework or entertainment to the observatory to occupy that period. If you're

not sure where the observatory is check out the links at `www.physics.csbsju.edu/astro`. Also on that page, check out the "Sky weather prediction for SJU Observatory". This link to the "Clear Sky Chart" has proven to be the best of many poor predictors of sky conditions. Look for the raw data frames to appear on the linux filesystem in the directory `/ccd/`*YYMMDD*`lab`, e.g., pictures taken during the evening of 4th of July would be in `/ccd/170704lab`.

Note: We will be taking several (often three) duplicate frames through the four different filters. Between object frames, darks, and flats typically ∼100 pictures are taken.

Example 1: Plan for Lunar Month starting 21-July-2005

Immediately on starting `xephem`, `Set` the location: SJU Observatory, click on the `Calendar` for the following <u>new</u> moon ("NM", in this case 4-August-2005) and enter a `Local Time` of 21:00 (9 P.M.). Hit `Update` so `xephem` is ready to display the sky at that time. `View→Sky View` then displays the night sky for that location/date/time. (Print a copy of this sky view as described in `using.xephem.txt` and record: `UTC Time: 2:00`, `Sidereal: 16:37`.) IC 4665 is the obvious target; its RA (listed in Table 4.2) is most nearly equal to the sidereal time and hence it is near the meridian, However, with a diameter of $70'$, IC 4665 is much larger than the ST7 CCD frame, so only a small fraction of it will be imaged—a fraction that must include several calibrated stars. A visit to the IC 4665 cluster web page[37] finds a couple of dozen of VRIc observations. I copy and paste that data into a spreadsheet, and then seek corresponding UBV CCD data. The result is 12 stars with the full set of $BVRI$ data. Next we need to find a CCD frame that will include as many of these stars as possible. (It is of course possible to use a different set of stars to calibrate different filters, but it will be easier if one set of stars will serve for all calibrations.) Surprisingly, most of the 12 stars have SAO[38] identifications; only three stars must be located by RA and dec. `Aladin` can find a low magnification ($1.5° × 1.5°$) image of IC 4665. (Print this image as a low magnification finder chart.) A request to VizieR for the SAO catalog objects near IC 4665 allows me to locate the calibrated sources found above. Since IC 4665 is much larger than our CCD frame, we aim for the largest possible subset of these stars. A CCD frame centered near SAO 122742 will pick up four fully calibrated stars (73, 82, 83, 89). Simbad gives $B-V$ data for several other bright stars in this frame (e.g., TYC 424-75-1, Cl* IC4665 P44), but I don't find additional $R-I$ data in Simbad. Returning to `obswww.unige.ch`, I find (depending on the exact position of the CCD frame) it may be possible to include $R-I$ calibrated stars 67, 76, 84, & 90. You should decide exactly how to place the CCD frame and locate the calibrated stars on a finder chart that is about 2× the size of the CCD frame. For focus stars consider SAO 122671 (mag=3) and SAO 123005 (mag=5). Note that SAO 122723 would make a good (bright: mag=6.8) star to aim the LX200 near this object. (I call such aiming/finding stars 'LX200 stars'. The LX200 object library includes all SAO stars brighter than magnitude 7, but any bright star can help assure the telescope is aimed at what you intend (and that the telescope's reported RA/dec are accurate). You can load the SAO_LX200.edb database into `xephem` to display the LX200 stars; SAO_mag75.edb includes about twice as many stars (down to magnitude 7.5); SAO_full.edb includes about a quarter of a million stars (down below magnitude 9).

---

[37]`http://obswww.unige.ch/webda/`
[38]Smithsonian Astrophysical Observatory—a standard catalog of 'bright' stars.

In such a large cluster, it would be wise to select additional fields, for example one centered near SAO 122709. A CCD frame there might include $R - I$ calibrated stars: 39, 40, 43, 44, 49, 50, 58, 62.

To select alternative standards… WIYN has a web page[39] with recommended standard star regions. (WIYN's stars are designed for a large telescope, and hence would require long exposures on our telescope). Peter Stetson's extensive list of standards is also online[40]. The `xephem` databases LONEOS.edb, Landolt83.edb and Buil91.edb contain shorter lists of brighter stars: < 13mag, ~ 9.5mag and < 8mag respectively.) Generally these good standard stars will be well-separated from the target, so air mass air mass correction would be required. (Since I have internal 'calibrated' sources, I'm not required to take CCD frames of these standards, however I've decided to 'be prepared' and hence have recorded the basic data I would need to observe them.) I select: #109 (PG1633+099, at RA=16:35, LX200 star: SAO 121671), #121 (110 506, at RA=18:43, LX200 star: SAO 142582), and #125 (111 1969, at RA=19:37, LX200 star: SAO 143678, also see: SAO 124878). These standard stars can be marked as `xephem` Favorites from the UBVRI.edb database. These sources should span a good range of air mass in the general direction of the target. Following the instructions in `using.xephem.txt`, I create a file of basic location data for my target and standard fields. By default, this file is: `.xephem/datatbl.txt` and can be printed (`% lp` *filename*) or edited (`% kwrite` *filename*).

Example 2: Plan for Lunar Month starting 19-August-2005

After Setting `xephem` for location: SJU Observatory, the new moon date 3-September-2005, and Local Time 21:00 (9 P.M.), I find and record: UTC Time: 2:00, Sidereal: 18:35. NGC 6633, whose RA is most nearly equal to the sidereal time and hence is near the meridian, is the obvious target. After adding NGC 6633 to `xephem` Favorites and loading the SAO database (Data→Files; Files→SAO_mag75.edb), it's easy to zoom in (lhs scroll bar) on NGC 6633 and find the nearby bright (5.7 mag) star SAO 123516[41], which would be a good star to steer the LX200. For focus stars consider SAO 122671 (mag=3) and SAO 123377 (mag=5). A visit to the NGC 6633 cluster web page[42] finds six VRIe observations for R. Cross-reference shows that all six are ~ 8 mag SAO stars[43], however only two (50 & 70) are in the central region of the cluster. (They could also be found using SAO_full.edb.) Stetson reports BVI data for NGC 6633, however the brightest ten of his stars are ~ 13 mag, which is $100\times$ dimmer than the ~ 8 mag R-mag stars. Thus different frames are required to properly expose the Stetson standards and the R 'standards'.

Using the Buil91.edb database, I can find bright standard stars: SAO 085402, SAO 141956, SAO 145050. These bright SAO stars are themselves LX200 stars.

---

[39] http://www.noao.edu/wiyn/obsprog/images/tableB.html

[40] http://cadcwww.hia.nrc.ca/standards

[41] VizieR reports $R = 5.703$, for this star, which may serve as an additional standard. FYI: this star is also known as: HD 170200 and HR 6928.

[42] Again: http://obswww.unige.ch/webda/

[43] These dim SAO stars are not in SAO_mag75.edb so I located them using `Aladin`

Example 3: Plan for Lunar Month starting 21-June-2005

After Setting `xephem` for location: SJU Observatory, the new moon date 6-July-2005, and Local Time 22:00 (10 P.M. — it's not dark at 9 P.M.), I find and record: UTC Time: 3:00, Sidereal: 15:43. Because of its larger declination, Upgren 1 has a bit less air mass than NGC 6633, so it becomes the target. Upgren 1 is not in `xephem`'s databases, so it must be added to Favorites following the procedure recorded in `using.xephem.txt`. A visit to the Upgren 1 cluster web page[44] finds seven stars with VRIc and UBV observations. However the color index disagreements are of order 0.05, so we can use this as an opportunity to find the correct values. Using the Landolt83.edb database, I find three neighboring standard stars with a range of colors: HD 102056 (LX200 star: SAO 81968, bluer than the Upgren 1 stars), HD 106542 (LX200 star: SAO 100009, redder than the Upgren 1 stars), and HD 107146 (LX200 star: SAO 100038, similar to the Upgren 1 stars). Using the Oja96.edb database, I find two very close stars with similar colors: BD+35 2356 and BD+34 2338. (For these dimmer, $\sim$10 magnitude, stars finder charts are required.) $*$#133 (SAO 63257, with mag 5 partner 63256) is a neighboring mag 3 star, SAO 44230 is a mag 4 star — both can help focus and alignment. SAO 63118 is the nearest LX200 star to Upgren 1 (since Upgren 1 is not in the LX200 catalog of clusters, the final jump must be made based on RA/dec). All but one of the Upgren 1 seven stars is an SAO star; they are all easy to identify with `Aladin`. (FYI: spiral galaxies M94 and M63 might be worth a look.)

Target and standards were fairly close together and near the meridian during the measurements, with airmass varying from 1.01 to 1.14. This was not a sufficient range to detect airmass correction terms. Increasing airmass dims and reddens stars. As a result calibrated stars viewed through a larger air mass will have a smaller constant in the color calibration equation Eq. 4.44. In this case, stars at airmass 1.14 were used to determine the color calibration equation which was then applied to unknown stars at airmass 1. The result is a bias in the estimated color of the unknown stars: their actual $B - V$ is likely to be bigger than that calculated using the calibration equation (i.e., color calibration constant should be larger at airmass 1). The effect can probably be ignored for Δairmass$\sim$0.1; Adjusting for this effect (e.g., determining[45] the term B in Eq. 4.37) typically requires measuring stars with Δairmass$\sim$1.

Sample Data

The large open cluster IC 4665 was the target for two nights during August 2010. The results are reported in Figure 4.14.

Report Checklist

1. Write an introductory paragraph describing the basic physics behind this experiment. For example, why does smaller (even negative) $B - V$ correspond to higher temperature? Why do we expect $v - V$ to be approximately constant? (This manual has

---

[44] Again: `http://obswww.unige.ch/webda/`

[45] On a following night, stars from IC 4665 were used to provide high airmass data. The results were: $B - V = 1.30(b - v) - .59 - .09 \sec z$, $R - I = .85(r - i) + .84 - .06 \sec z$

Names	Constellation	Right Ascension (2000)	Declination (2000)	Diameter (arcmin)	Reddening (mag)
M34, NGC 1039	Per	$02^h42^m05^s$	$+42°45'42"$	25	0.07
IC 348	Per	03 44 30	+32 17 00	10	0.93
Collinder 69	Ori	05 35 06	+09 56 00	70	0.10
M35, NGC 2168	Gem	06 09 00	+24 21 00	25	0.26
NGC 2264, cone	Mon	06 40 58	+09 53 42	40	0.05
NGC 2301	Mon	06 51 45	+00 27 36	15	0.03
NGC 2420	Gem	07 38 24	+21 34 49	10	0.05
M67, NGC 2682	Cnc	08 51 18	+11 48 00	25	0.06
Upgren 1 (asterism)	CVn	12 35 00	+36 18 00	15	
M5, NGC 5904	Ser	15 18 33	+02 04 58	23	0.03
IC 4665	Oph	17 46 18	+05 43 00	70	0.17
NGC 6633	Oph	18 27 15	+06 30 30	20	0.18
NGC 6738 (asterism)	Aql	19 01 21	+11 36 54	30	
NGC 6823	Vul	19 43 12	+23 18 03	12	0.86
NGC 6940	Vul	20 34 32	+28 15 08	31	0.25
M52, NGC 7654	Cas	23 24 33	+61 36 58	13	0.65
NGC 7790	Cas	23 58 24	+61 12 30	17	0.53

Table 4.2: Candidate targets. `http://obswww.unige.ch/webda/` and *Allen's Astrophysical Quantities* p. 548 have lists of clusters. An ideal candidate would be within telescope range (Dec: $-5° < \delta$), a size that matches our camera ($\sim 15'$), have little reddening, and contain calibrated sources.

Label	Name	SpType	$b-v$	$r-i$	$B-V$	$R-I$	T_B (K)	T_R (K)
			16 August 2010					
A	TYC 424-648-1	G8	1.260	0.198	1.278	0.600	4054	4506
B	IC 4665 93	G5	0.922	0.024	0.858	0.447	5083	5089
C	TYC 428-1938-1	A	0.644	−0.151	0.505	0.305	6218	5894
D	TYC 428-691-1	A3V	0.518	−0.258	0.349	0.210	6900	6680
			17 August 2010					
A	TYC 424-648-1	G8	1.273	0.256	1.252	0.642	4112	4379
B	IC 4665 93	G5	0.951	0.007	0.844	0.425	5122	5189
C	TYC 428-1938-1	A	0.719	−0.165	0.553	0.258	6038	6252
D	TYC 428-691-1	A3V	0.571	−0.189	0.361	0.237	6839	6427

Table 4.3: The instrumental color indices: $b-v$ and $r-i$ of the 'unknown' stars in IC 4665 were measured using `gaia` and converted to standardized color indices: $B-V$ and $R-I$ using the calibration lines displayed in in Figures 4.14c and 4.14d. Eq. 4.28 (T_B) and Eq. 4.29 (T_R) were used to calculate the temperature of the stars from each color index. The night-to-night variation in the color indices is about .035 mag; almost certainly this variation is a measurement error not a real change in the stars. Note that this error is larger than that suggested by the statistical error reported by `gaia` (~ 0.005 mag) in the standard stars. (The dimmer 'unknown' stars had statistical errors ~ 0.01 mag.) The two temperatures T_B and T_R do not exactly agree; as discussed in the text systematic errors of a few percent are to be expected.
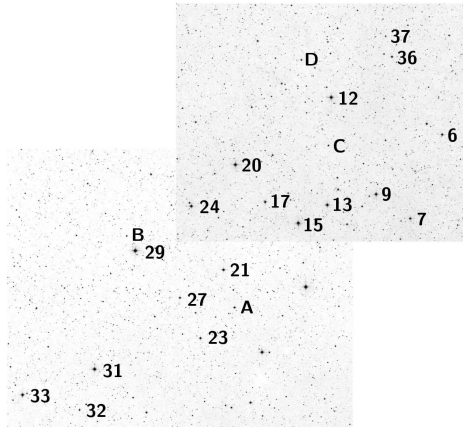
(a) This Digitized Sky Survey image shows the central $\sim 50' \times 45'$ region of the open cluster IC 4665. The standard stars of J.W. Menzies and F. Marang (MNRAS, 282, 313–316 (1996)) are labeled along with three 'unknown' stars: A, B, C, D.
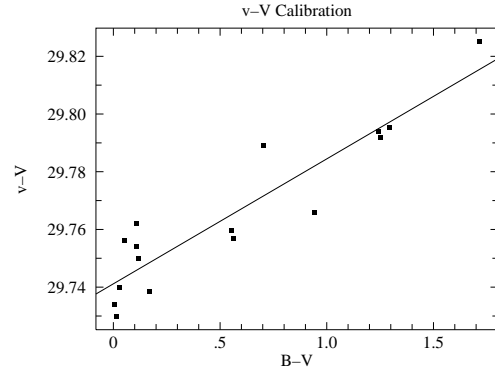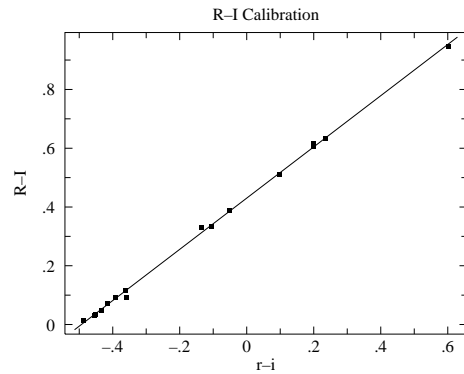

(b) The total color correction in this data set is approximately 0.1 mag. The deviation about this color corrections curve is about 0.01 mag. See Eq. 4.42.

$v - V = 29.74 + 0.04(B - V)$.
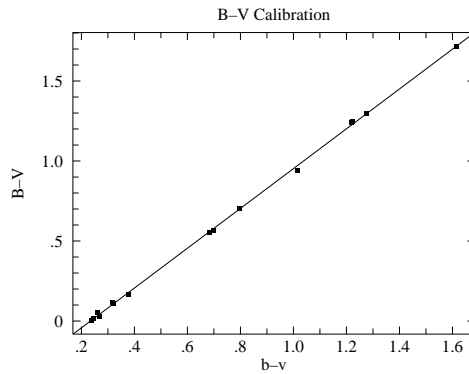
(c) Calibration of the standardize color index $B - V$ in terms of the instrumental color index $b - v$. See Eq. 4.44. The rms deviation from this calibration is about 0.014 mag.

$B - V = -0.29 + 1.24(b - v)$

(d) Calibration of the standardize color index $R - I$ in terms of the instrumental color index $r - i$. The rms deviation from this calibration is about 0.01 mag.

$R - I = 0.43 + 0.87(r - i)$

Figure 4.14: Two frames were used to image the central region of the open cluster IC 4665 on 16-Aug-2010. This region includes 16 standard stars which were used to calibrate the relationships between standardized color indices and instrumental color indices. Using these relationships and the measured instrumental color indices, we can determine the standardized color indices of any star in the imaged region. The area was re-imaged the following night producing two sets of results for the unknown stars as reported in Table 4.3. Note: the reported 'rms deviation' is the square root of *WAPP*⁺'s 'reduced chi-square' since neither x or y errors were entered.

many pages on these topics; your job is condense this into a few sentences and no equations.) Recall notation: lower case letters (b, v, r, i) represent the 'instrumental' magnitudes you get using `gaia` to analyze your images. Upper case letters (B, V, R, I) represent the 'book' or standard magnitudes.

2. Files containing the reduced frames and object frames for your cluster in FIT format (usually three repeats for each filter). Leave these in your linux account, but identify the filenames (and folder) in your notebook. While basic frame characteristics (filter, exposure time, date/time of exposure, . . .) are contained in each file, you should also record this information in your notebook. (The command: `fitshead *F.FIT` will display this information from the `*F.FIT` files in a format that allows easy copy & paste.)

3. Files containing the flat-field frames you used to flat-field your images. (One for each filter, but perhaps derived as an average of several frames.) Leave these in your linux account, but record the filenames and characteristics in your notebook.

4. Hardcopy finder charts, with your target, calibrated stars and unknown stars labeled. (Similar to Figure 4.14a.) Record an RA/dec grid on your finder charts.

5. `xephem` datafile containing basic data (RA, Dec, altitude, air mass for each observation night). Print this out and tape in your lab notebook.

6. Table containing the basic data on your calibrated stars, including standard names and magnitudes. (Perhaps included in the below file.)

7. A spreadsheet file, reasonably well documented, containing known and instrumental magnitudes of the standard stars and the instrumental magnitudes of several unknown stars. Note that usually you will have three full repeats of this data. Calculate instrumental color indices $(b - v$ & $r - i)$. For the standard stars calculate instrumental−standard magnitude $(v - V)$ and record the basic statistics (mean, standard deviation) for those standard stars for each repeat. (Note that aside from a smallish color correction, we expect $v - V$ to be constant.) Data from this spreadsheet will be used in the below fits and calculations. Remember to self document all these calculations before you print out the data table for inclusion in your notebook.

8. Linear fits of $B - V$ vs. instrumental $b - v$ for each of your three sets of standard star data. You will need—and so your spreadsheet should record—results (A, B, χ^2) for all fits, however print out the fit report only for the fit you consider 'best'. Make a hardcopy plot of that 'best' $B - V$ vs. instrumental $b - v$ data set with a fitted line. (Similar to Figure 4.14c.) (General rule: include a hardcopy fit report for every plot!) FYI: I would make a big concatenated `log.txt` file containing anything that might be important in the future. I've had to learn the hard way that repeating lost calculations takes time whereas copy & paste of results is nearly instantaneous.

9. Typically you will have three repeats of $(r - i, R - I)$ datasets. As above, separately fit each data set and record results (A, B, χ^2) for all fits. Print out the fit report only for the fit you consider 'best'. Make a hardcopy plot of $R - I$ vs. instrumental $r - i$ with a fitted line for that 'best' fit. (Similar to Figure 4.14d.)

10. Typically you will have three repeats of $(B - V, v - V)$ datasets. As above, separately fit each data set and record results (A, B, χ^2) for all fits. Print out the fit report only

for the fit you consider 'best'. Make a hardcopy plot of $v - V$ vs. known $B - V$ with a fitted line. (Similar to Figure 4.14b.)

11. Three repeats of: calculation of the $B - V$ of several unknown stars based on the unknown stars' $b - v$ and the corresponding linear fit made using standard stars in the same frames in #8 above. The best estimate of a star's $B - V$ will of course be the average of the three repeats for that star, but what should be recorded as the uncertainty? One option would be the standard deviation of the three values. However, the typical deviation of the standard stars used in making the fit would also show expected deviation. When no errors are supplied to $WAPP^+$, the reduced chi-square it reports is simply the average deviation squared:

$$\text{reduced } \chi^2 = \frac{1}{N-2} \sum (\Delta y_i)^2 \tag{4.45}$$

Thus the square root of the reduced chi-square immediately gives you something like the average (rms) deviation of the points used in the fit. A conservative choice for uncertainty would be the larger of the above two methods.

12. Analogous to the above, calculation of the $R - I$ of several unknown stars based on the unknown stars' $r - i$ and the corresponding linear fit made using standard stars in the same frames as in #9 above. As above, record an error estimate for the $R - I$ of those unknown stars.

13. Analogous to the above, calculation of the $v - V$ of several unknown stars based on the unknown stars' $B - V$ (which you calculated in #11 above) and the corresponding linear fit made using standard stars in the same frames in #10 above. Clearly: $V = v - (v - V)$ allows three calculations of an unknown star's V magnitude, but what should be recorded as an uncertainty in the average value? Again, standard deviation provides one answer. The error in $v - V$ can be estimated from the square root of the reduced chi-square, but that error should be combined in quadrature with the error in v. If we guess that the error in v is comparable to the error in $v - V$, we end up with an error estimate in V as $\sqrt{2}\times$ the square root of the reduced chi-square. Again, a conservative choice for uncertainty would be the larger of the above two methods.

14. Calculation of the temperature (T_B, see Eq. 4.28) of several unknown stars based on $B - V$. (See Table 4.3.) Given an error for $B - V$, the 'high-low' method will allow you to propagate that $B - V$ error into a T_B error.

15. Similar to previous item, calculation of the temperature (T_R, see Eq. 4.29) with error of those same stars based on $R - I$.

16. A properly formatted (units, errors, sig figs) final results table displaying V, $B - V$, $R - I$, T_B, T_R (all with errors) for your unknown stars (i.e., somewhat similar to Table 4.3, but with errors). Are T_B and T_R consistent? Comment on the uncertainty in temperature. What do you believe are the major sources of uncertainty?

Other Projects

The lab is aimed at one fairly simple project: measuring stellar magnitudes using in-frame calibrated stars. However, the techniques discussed here can be applied to a variety of other projects, some of which are listed below.

1. Imaging of extended objects (galaxies, nebulae, planets,...)

2. Orbit determination of Solar System objects (moons, comets, asteroids,...)

3. Magnitude as a function of time

   (a) Pulsing stars: Delta Scuti (`http://www.astro.univie.ac.at/~dsn/`), RR Lyrae, Cepheids

   (b) Cataclysmic variables (`http://cba.phys.columbia.edu/`)

   (c) Eclipsing binaries (`http://www.rollinghillsobs.org/`)

   (d) Novae and supernovae

   (e) Rotation period of an asteroid

   (f) American Association of Variable Star Observers (`www.aavso.org`) projects

4. Careful determination of any significant parameter of the telescope system (e.g., S/N issues, atmospheric extinction, color corrections, tracking, ...)

References

1. Santa Barbara Instrument Group (`www.sbig.com`), *Operating Manual* for STL-1001E, `STL_Operating_Manual.pdf`

2. Santa Barbara Instrument Group (SBIG), *Users Guide* for CCDOps Version 5 `CCDops_v5.pdf`

3. Meade (`www.meade.com`), *Instruction Manual* for 12" LX200 `LX200_Classic_Manual.pdf`

4. Howell, Steve B., *Handbook of CCD Astronomy*, Cambridge, 2000

5. Howell, Steve B., *Astronomical CCD Observing and Reduction Techniques*, ASP Vol. 23 1992

6. Buil, Christian, *CCD Astronomy*, Willmann-Bell, 1991

7. Romanishin, W. *An Introduction to Astronomical Photometry Using CCDs*, 2006 `http://observatory.ou.edu`

8. J. Palmer & A.C. Davenhall [starlink], *The CCD Photometric Calibration Cookbook*, `starlink_ccd.pdf`

9. ed. Cox, Arthur N., *Allen's Astrophysical Quantities*, AIP/Springer, 2000

10. American Association of Variable Star Observers (`www.aavso.org`), *CCD Manual* `aavso_ccdmanual.pdf`

Appendix: Available Sloan Filters: $g'r'i'$

The Sloan Digital Sky Survey is an ambitious project to deeply image and reduce a large fraction of the sky. The imaging is done in 5 new filters[46] $u'g'r'i'z'$; our camera has available the central filters: $g'r'i'$. Figure 4.15 displays the characteristics of these filters.

Most any deeply exposed frame in the region imaged by SDSS will include stars[47] with cataloged[48] photometry accurate to approximately $\pm.03^m$. While this error is $\sim 10\times$ larger than the usual $UBVRI$ standard stars, it is adequate for this lab. Unfortunately, many open clusters are not in the region imaged by SDSS (because the focus of the project is objects beyond our Galaxy.) These Sloan magnitudes are based on the AB_ν system rather than the Vega system. Instead of the star Vega defining magnitude=0, it is intended that, for each filter, magnitude=0 corresponds to $F_\nu = 3631$ Jy. The results are not hugely different from Vega-based systems: $g = -.08$, $g - r = -0.25$, $r - i = -0.23$ for Vega.

Various transformations of $BVRI \iff g'r'i'$ for normal stars have been published[49], I reproduce a few of these results below:

$$B - g = 0.313(g - r) + 0.219 \tag{4.46}$$
$$V - g = -0.565(g - r) - 0.016 \tag{4.47}$$
$$R - r = -0.153(r - i) - 0.117 \tag{4.48}$$
$$i - I = 0.247(R - I) + 0.329 \tag{4.49}$$
$$r - i = 1.007(R - I) - 0.236 \tag{4.50}$$
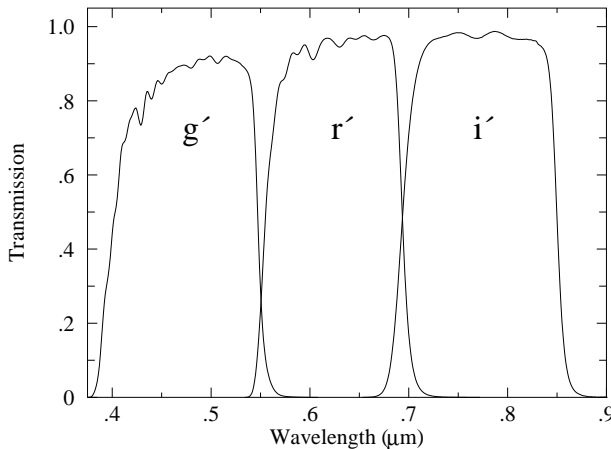
| Filter Name	λ (μm)	$\Delta\lambda$ (μm)	F_0 (W/m^2 μm)
g'	.46	.13	4.71×10^{-8}
r'	.61	.12	2.81×10^{-8}
i'	.74	.12	1.87×10^{-8}

Figure 4.15: The characteristics of the Sloan filters: g' (green), r' (red), i' (infrared) from the Gemini Observatory: http://www.gemini.edu and Annual Review Astronomy & Astrophysics (2005, Bessell)

---

[46]Fukugita, M., Ichikawa, T., Gunn, J. E., et al. 1996 AJ, 111, 1748

[47]The brightest stars recorded will have mag=14, which in the context of our telescope, are dim. For r' and i' use exposure times ≥ 120 s. For g' use exposure times ≥ 300 s.

[48]http://www.sdss.org/

[49]Jordi, K.; Grebel, E. K.; Ammon, K. A&A **460** 339 (arXiv:astro-ph/0609121)
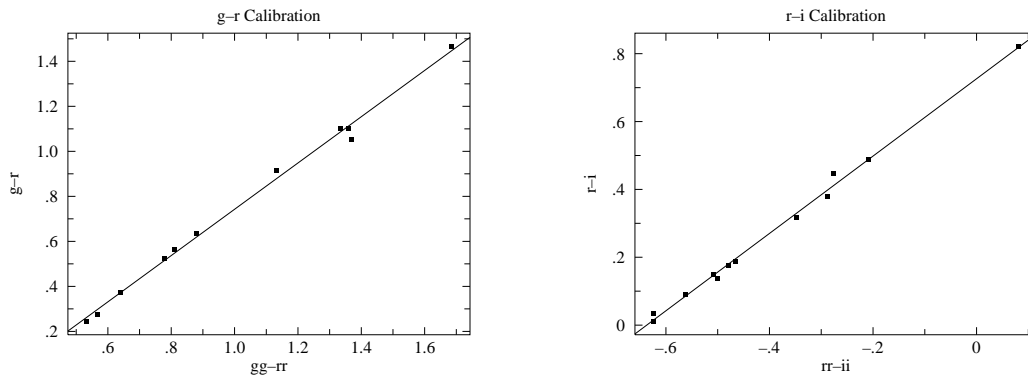
(a) Calibration of the standardize color index $g - r$ in terms of the instrumental color index $gg - rr$. See Eq. 4.44. The rms deviation from this calibration is about 0.03 mag.

$g - r = -0.29 + 1.03(gg - rr)$

(b) Calibration of the standardize color index $r - i$ in terms of the instrumental color index $rr - ii$. The rms deviation from this calibration is about 0.015 mag.

$r - i = 0.73 + 1.14(rr - ii)$

Figure 4.16: Two identical frames (taken 16-Aug-2010) of the central region of the open cluster NGC 6791 were used to calibrate the relationships between standardized color indices and instrumental color indices . This region includes 12 standard stars ($BVRIgri$).

Appendix: ST-7E Camera

In June 2009 we 'retired' the old but fully functional SBIG ST-7E camera. I've dumped the specifications for this camera in this Appendix as it is possible that it might be returned to service. Flaws in the CCD are most evident in the bias frame[50]. Measurements on our CCD shows that the difference between two bias frames shows an approximately normal distribution (aside from the flaws) with a standard deviation ~ 6 ADU. Also note that the system artificially introduces an offset of 100 into each pixel, so $\frac{2}{3}$ of the pixels in a bias frame are expected in the range 100 ± 6 ADU. The ST-7 uses a thermoelectric cooler which can cool the CCD $\sim 30°$C below ambient temperature, reducing the dark currents by about a factor of 10. The resulting dark currents are *not* negligible for exposures longer than a few minutes.

---

[50]Our CCD has a flaw at pixel $(592, 194)$ which affects the entire 592 column

Telescope	Meade LX200		CCD	Kodak KAF-0401E
aperture	12"		pixel	$9\ \mu\text{m} \times 9\ \mu\text{m}$
focal ratio	$f/10$		full-well	$\sim 50,000\ e^-/\text{pixel}$
focal length	120"		read noise	$15\ e^-$ rms
Focal Reducer	Meade f/3.3 FR/FF		gain	$2.3\ e^-/\text{ADU}$
effective f	50"			
Filter Wheel	SBIG CFW-8A		λ	Quantum Efficiency
Camera	SBIG ST-7E ABG		$.65\ \mu\text{m}$	60%
pixels	765×510		$.55\ \mu\text{m}$	50%
image	$18' \times 12'$		$.45\ \mu\text{m}$	40%
scale	1.45"/pixel		$.40\ \mu\text{m}$	30%

Table 4.4: Older CCD photometry equipment available at the SJU observatory. Note: When combined with a Celestron f/6.3 FR/FF this camera yielded 0.97"/pixel; when used on the 10" Meade telescope without any FR/FF it yielded 1.07"/pixel.

The large open cluster IC 4665 was the target for two nights during August 2005. The results are reported in Figures 4.19 and 4.20.

During the first night an overlapping mosaic of five frames was used to image the central region of the cluster. During a 2 hour period $BVRI$ frames were taken at each pointing. (During this time the air mass to IC 4665 changed from 1.30 to 1.46, but the data show no sign of a change in the transparency of the atmosphere, so no air mass corrections were applied.) Dome flat-field frames (taken 12 hours earlier) were used to produce reduced frames. `gaia` was used to measure the instrumental magnitude of 18 standard stars and three 'unknown' stars. The magnitudes were pasted into a `gnumeric` spreadsheet which was used to calculate the color indices: $b - v$ and $r - i$. (Since overlapping fields were used typically a standard star appeared in a couple of frames. When this occurred average instrumental color indices were used.) A calibrating line relating the standard stars' known $B - V$ and the measured $b - v$ was fit using regression in `gnumeric`. An identical process was used to find the relationship between $R - I$ and $r - i$. The results are displayed in Figures 4.19c and 4.19d. Using these relationships and the measured instrumental color indices, we can determine the standardized color indices of any star in the imaged region. As shown in Table 4.5, Eq. 4.28 or Eq. 4.29 can then be used to find the temperature of each 'unknown' star.

During the second night six (generally not overlapping) frames were selected with the aim of capturing a diverse (hot and cool) set of standard stars. The data collected during this night *did* show a change in the transparency of the atmosphere (there was a larger variation in air mass: 1.32 to 1.63; see Figure 4.20a), so air mass corrections were applied.
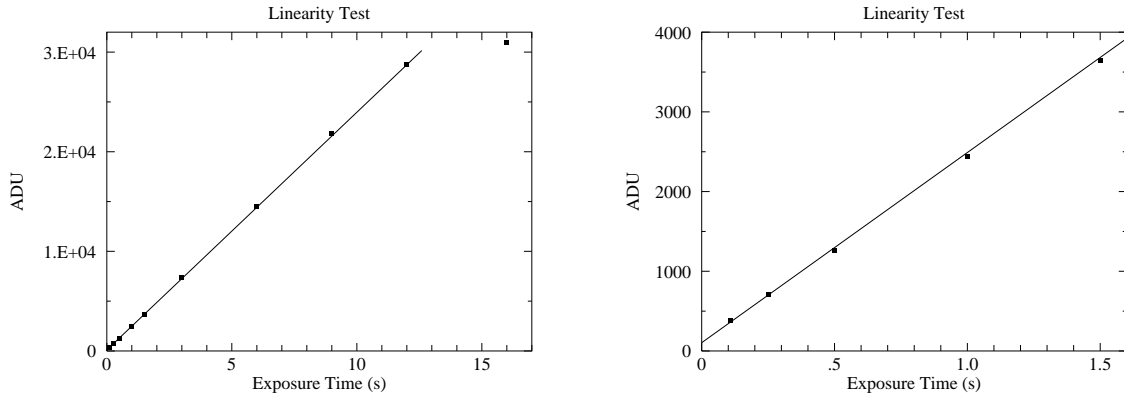
Figure 4.17: Below $\sim 30,000$ ADU (12 second exposure) the response of our CCD seems to be linear, with saturation quite evident in the 16 second exposure. In fact, the CCD should not be trusted to be linear above $\sim 25,000$ ADU.

The linear fit may look good, but it is in fact not great: reduced χ^2=8. Systematic error in the shutter speed control is probably a problem for the short exposures. (Elimination of the two shortest exposures results in a reduced χ^2=1.6.) Also note that the y intercept is not exactly zero: with this camera zero-time exposures are designed to produce an output of about 100 ADU.

Label	Name	SpType	$b-v$	$r-i$	$B-V$	$R-I$	T_B (K)	T_R (K)
A	BD+05 3486	A2	0.404	-0.708	0.2822	0.1826	7255	6966
B	GSC 00428-00981	G5	0.833	-0.387	0.8399	0.4625	5133	5015
C	TYC 424-517-1	K5	1.047	-0.151	1.1181	0.6683	4421	4306

Table 4.5: The instrumental color indices: $b-v$ and $r-i$ of the 'unknown' stars in IC 4665 were measured using `gaia` and converted to standardized color indices: $B-V$ and $R-I$ using the calibration lines displayed in in Figures 4.19c and 4.19d. Eq. 4.28 (T_B) and Eq. 4.29 (T_R) were used to calculate the temperature of the stars from each color index. The two temperatures do not exactly agree; as discussed in the text systematic errors of a few percent are to be expected.
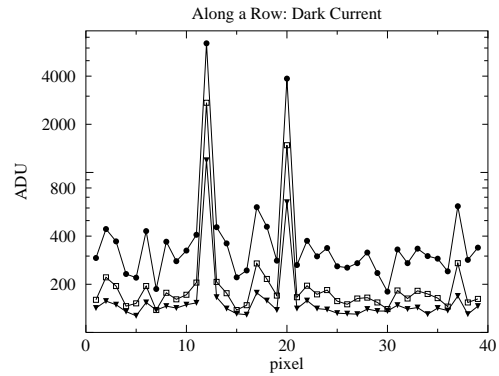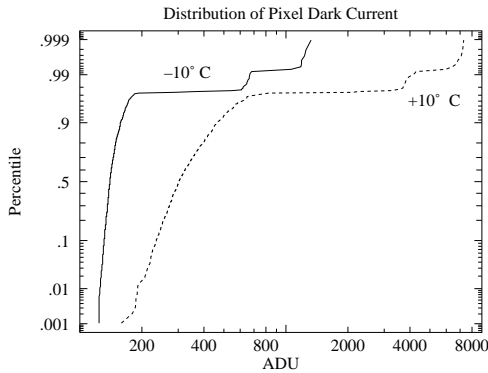
(a) The distribution of pixel dark current at $+10°$C and $-10°$C. All but a few of the pixels have a (log)normal distribution of dark current. A few percent of the pixels show much larger dark current: these are the 'hot' pixels. Note that both classes of pixels respond to temperature: lowering the temperature reduces every pixel's dark current.

(b) Part of a row of pixels is displayed at three temperatures: ● = $+10°$C, □ = $0°$C, ▼ = $-10°$C. Isolated hot pixels are randomly sprinkled throughout the image (here at columns 12 and 20). The data here and in (a) are from 15 minute dark frames.
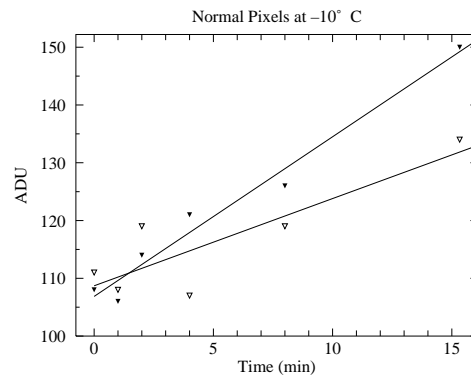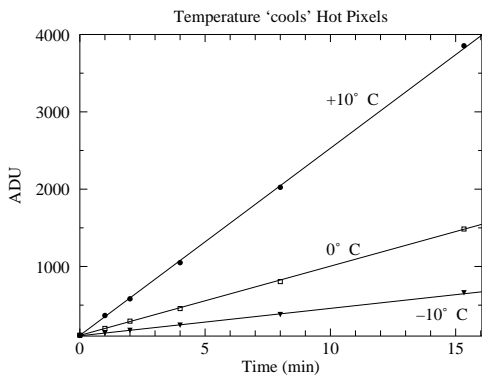
(c) Dark current produces ever larger stored charge in a pixel; of course reducing the temperature reduces the dark current.

(d) While it is more evident in this low count data, there is always deviation in counts. While we can subtract the average dark charge, deviations from the average produce 'noise' in our images. Reducing the temperature reduces this noise.

Figure 4.18: Dark frames are 'exposures' with the shutter closed. The source of these counts is not starlight, rather a thermally induced current allows charge to accumulate in each pixel. This 'dark current' can be exceptionally large in 'hot pixels'.
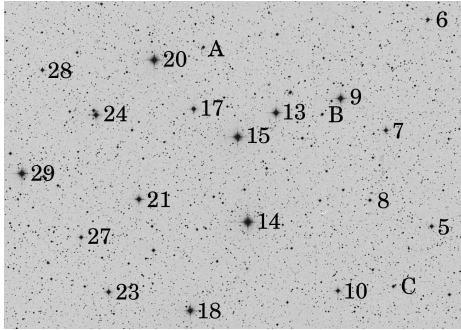
(a) This Digitized Sky Survey image shows the central $\sim 50' \times 25'$ region of the open cluster IC 4665. The standard stars of J.W. Menzies and F. Marang (MNRAS, 282, 313–316 (1996)) are labeled along with three 'unknown' stars: A, B, C.
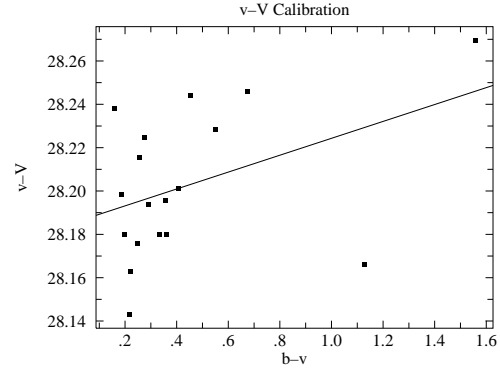
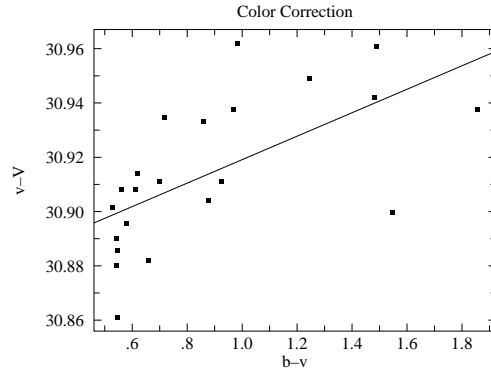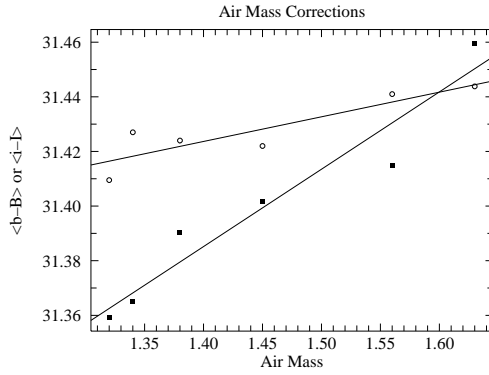(b) There is little evidence for a significant color correction in this data set. See Eq. 4.42.
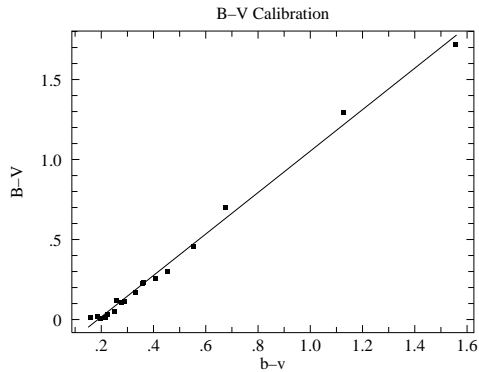
(c) Calibration of the standardize color index $B - V$ in terms of the instrumental color index $b - v$. See Eq. 4.44.
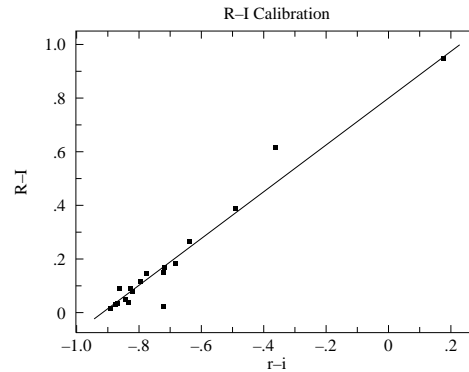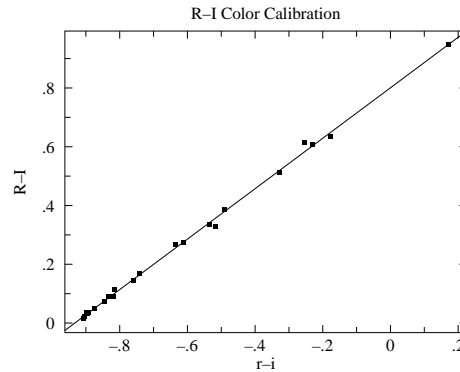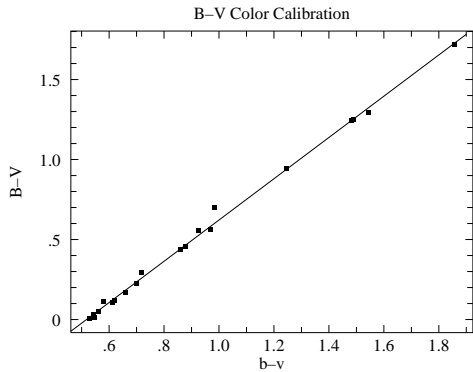

(d) Calibration of the standardize color index $R - I$ in terms of the instrumental color index $r - i$.

Figure 4.19: An overlapping mosaic of five frames was used to image the central region of the open cluster IC 4665. This region includes 18 standard stars which were used to calibrate the relationships between standardized color indices and instrumental color indices. Using these relationships and the measured instrumental color indices, we can determine the standardized color indices of any star in the imaged region.

Air Mass Corrections

Color Correction

(a) Short wavelengths are more affected by atmospheric absorption than long; the above shows the effect on B magnitudes (filled squares) and I magnitudes (open circles). The y axis displays the difference between instrumental and standardized magnitudes averaged over all the blue stars in the frame.

(b) Color correction is evident in this data set, but both air mass and color correction should be applied to this data. This full result was: $v - V = 30.611 + 0.179 \sec z + 0.048(b - v)$. The rms variation from this line was less than 0.02 mag.

B–V Color Calibration

R–I Color Calibration

(c) Calibration of the standardize color index $B - V$ in terms of the instrumental color index $b - v$.
$B - V = -0.67 + 1.29(b - v)$

(d) Calibration of the standardize color index $R - I$ in terms of the instrumental color index $r - i$.
$R - I = 0.80 + 0.86(r - i)$

Figure 4.20: Six frames were used to image 22 standard stars in the open cluster IC 4665. The selected stars have a wide variation in color in order to to achieve robust color calibrations. During the 2^+ hours of data collection the air mass increased from 1.32 to 1.63 and the resulting increase in atmospheric absorption increased (dimmed) B, V, R, and I magnitudes in proportion to the air mass (see Figure 4.20a).